"The Synchronizing and Monitoring System of the McGill Synchro-Cyclotron"

by

Ray W. Jackson

A Thesis submitted in partial fulfilment of the requirements for the degree of Doctor of Philosophy in the Faculty of Graduate Studies and Research,

McGill University.

McGill University,

Radiation Laboratory,

April, 1950.

TABLE OF CONTENTS

SUMMARY

The original contributions include a general survey of the problem of relating any event to the instantaneous frequency of a sweeping-frequency signal; the use of variable-frequency circuit analysis and the application of electronic circuit techniques in the design and construction of the apparatus of the requisite precision for synchronizing the cyclotron ion source pulse with the frequency-modulation cycle; the design and construction of a system for the convenient oscilloscopic monitoring of the cyclotron operation.

ACKNOWLEDGMENTS.

I wish to express special thanks to Professor J.S. Foster for his encouragement and assistance in the carrying out of this work; to Mr. P.B. Troup, electronics technician, for many helpful suggestions in the materialization of the ideas; to Mr. D.W. Hone and Mr. P.M. Milner for frequent helpful discussions; to Mr. J.F. Mathison for his expert and painstaking work in photographing the diagrams and oscilloscope traces; and to Mr. K.L.S. Gunn for invaluable last minute assistance.

CHAPTER I

INTRODUCTION

It is well known that the frequency of the r-f accelerating voltage in high energy cyclotrons must decrease with time to maintain resonance with the ions as their masses increase relativistically with energy. For this reason the frequency is continuously modulated by an approximately sinusoidal waveform and the ions are accelerated in bursts as the frequency repeatedly sweeps in the decreasing direction.

The ions formed by the ion source at the center of the magnetic field are accelerated over this decreasing-frequency sweep only if they are formed (or are still present) at the time when the frequency is passing through resonance with their natural orbital frequency in the central field. Ions released at other times in the modulation cycle serve only to unnecessarilyload the oscillator and wear out the ion source. Clearly an important problem is to pulse the ion source at the right moment in the f-m cycle and for a suitable length of time. The consideration of this problem has led to other related problems which have been grouped with it as the subject matter of this thesis.

Chapter II is concerned with the theory of the pick-up of ions into orbits and their acceleration to high energies, leading up to the calculation of the acceptance time (the effective resonance width for pick-up of ions into stable orbits) and thus to the estimation of the precision desired in the placing of the ion source pulse with respect to the instantaneous frequency of the accelerating voltage.

The modulation of the Dee voltage frequency is accomplished by a rotating condenser in the oscillator resonant circuit. The instantaneous frequency of the resulting voltage function may be approximately represented by(1)

$$\hat{f} = 24.4 - 3.6 \cos v\,t$$

where $\hat{f}$ = instantaneous frequency in Mc/s

v = modulating angular frequency in radians/s

$\frac{v}{2\pi}$ = 200 cps. for present operating conditions.

The region of resonance with ions at the center is a band of frequencies about $\frac{1}{4}$ Mc/s in width centered at 25.0 Mc/s. It is only over this region (about 60 μsec. in time) that ions at the center have a useful probability of being swept up into "phase-stable" orbits, and only over approximately the same range of frequency or time at the end of the accelerating frequency sweep that ions of full energy strike the internal probe target or, alternatively, pass between the deflecting electrodes. The positions of these periods with respect to the frequency modulation cycle are shown in fig. 1.

Chapter III and Appendix A are concerned with the relation of any event to the instantaneous frequency of the variable-frequency reference. In other language, the behaviour of the ions is entirely related to the sweeping-frequency driving function, the general character of which is expressible by the rotating vector

$$E(t) = E\, e^{j(\omega_o t - \epsilon t^2)}$$

The instantaneous frequency of this driving function is thus the only true reference for accurate measurements of the time or frequency at which events occur which concern the acceleration of ions. Because of inescapable vibration in the rotating condenser vanes and shaft, and finite machining errors (though as small as machining skill will practically allow) the instantaneous frequency reference cannot be accurately transformed to a linear time reference, or to an angular mechanical reference. It will be

apparent, for example, that any jitter in a trigger pulse generated at a certain point in the frequency sweep can be checked only by comparing it with another trigger pulse generated from the same frequency sweep in a similar way. The limitations on the possible accuracy of measurement of the instantaneous frequency of the above driving function by simple resonant circuits are discussed. It is pointed out that the consideration of the pick-up and acceleration of ions as a response to a sweeping-frequency driving function may lead to a better understanding of the mechanisms of ion acceptance and orbital phase-stability.

Chapter IV describes the circuits worked out and in use for synchronizing the ion source pulse and compares their performance with the previously worked out requirements. Other synchronized elements are briefly discussed in Chapter V.

The usefulness of the cyclotron as a research tool is determined to a great extent by the precision and ease of its adjustments. Thus the timing of the ion source pulse can be optimally adjusted only if the effects of varying its parameters are clearly presented. Towards this end the monitoring system described in Chapters VI and VII has been worked out. Special precautions were necessary to overcome the difficulties occasioned by the remote control operation of the cyclotron. The system is not perfect, as summarized in Chapter VIII, but it is felt that the main problems have been solved, laying the groundwork for further refinements as the need arises.

Incidental Note

The 82-inch McGill synchro-cyclotron is designed to accelerate protons to 100 Mev.

CHAPTER II

ION SOURCE PULSE REQUIREMENTS

1. Length.

In order to discuss the length and precision in placement required for the ion source pulse, it is necessary to know the length of time at the beginning of the acceleration sweep over which ions may be picked up and accelerated to full energy. The ions near the center, as they find the frequency of the accelerating electric field approaching their natural frequency of orbital rotation ω_o, will begin to pick up energy and move out from the center in widening orbits. Those starting too early or too late will find themselves gaining energy at the wrong rate and will slip out of phase with the changing frequency of the accelerating field. When this happens they have lost their chance to reach full energy on that acceleration sweep, and "the gang goes on without them".

The ion in the "equilibrium orbit", picked up at the center of the cyclotron at the exact instant when the r-f accelerating voltage across the gap is passing through the instantaneous frequency ω_o and the amplitude $V' \sin \varphi_s$, is a fiction which gains energy steadily in constant increments of $eV' \sin \varphi_s$ each time it crosses the gap until it reaches the target radius. Other ions, picked up in the central region over a limited range of frequencies earlier and later in the modulation cycle into "phase-stable" orbits are also accelerated to full energy, gaining or losing energy at the gap as their "gap-crossing phases" φ with respect to the Dee voltage oscillation execute "phase oscillations" about the value φ_s. The length of time Δt_{acc} over which acceptance of the ions at the center into phase-stable orbits

can occur is called the "acceptance time". It may be calculated approximately from some theoretical equations worked out by Bohm and Foldy[2]. In order to introduce the quantities and assumptions involved in the calculation, it is proposed to review briefly their treatment.

The natural frequency of an ion orbit at a given radius is determined by the ratio of charge to mass of the ion and the value of the magnetic field at that radius. The magnetic field is made to decrease slowly with radius to focus the orbits into the median plane, and the effective mass of the ion increases with radius as its velocity becomes comparable to the velocity of light; both these factors decrease the orbit frequency as the ion gains energy and moves in orbits of larger radius. If the ion is to gain energy in constant increments each time it crosses the gap, this required relation between frequency and orbit radius must be complied with by the relation between the rate of change of the applied frequency and the rate of energy gain impressed on the ion by the accelerating voltage. The interdependence of these quantities is expressed by the following equation, which holds for an ion in the equilibrium orbit at a radius which carries it out of the spatial extent of the accelerating field for most of its path (i.e., into the inside of the hollow Dee):

$$-\frac{1}{\omega_s^2}\frac{d\omega_s}{dt} = \frac{KeV \sin\varphi_s}{2\pi E_s} \qquad \text{.....(2.01)}$$

where ω_s = instantaneous angular frequency of ion in equilibrium orbit

K = a factor describing the magnetic field at any radius r.

$$= 1 + \frac{nc^2}{(1-n)v^2}$$

where v is the ion velocity

and $n = -\frac{r}{H}\cdot\frac{\partial H}{\partial r}$

e = charge on the ion

V = magnitude of the alternating accelerating voltage regarded

as applied at one gap per turn, or twice the magnitude of the r-f voltage on the Dee, V'.

φ = phase angle of the accelerating voltage at the instant the ion is crossing the gap. Energy gain of ion = $eV \sin\varphi$ per revolution.

φ_s = value of φ for ion in the equilibrium orbit.

E_s = total energy of ion in the equilibrium orbit.

The ion in the equilibrium orbit is assumed to gain energy at a constant rate $eV \sin\varphi_s$ per turn such that the phase angle φ_s is constant. The range of orbital frequencies about the equilibrium orbital frequency within which stable phase oscillations can occur is found to depend strongly on φ_s and is a maximum for φ_s approximately 30°. If φ_s is <u>not</u> constant over the acceleration sweep, it will be less than this optimum value at some point in the sweep, and orbits which satisfied the optimum stability conditions at the center might become unstable further out. Hence the effective acceptance time in terms of ions reaching the target might be less than that calculated for optimum conditions at the center. This has been considered by Henrich, Sewell, and Vale(3) but will not be gone into here. Here we shall understand by acceptance time the period of time for acceptance of ions into phase-stable orbits in the central region of the cyclotron - without regard to their fate later in the modulation cycle.

If we assume that φ_s is constant or changing very slowly, then φ_s is also the instantaneous angular frequency of the r-f accelerating voltage. We may picture the radial position vector of the general ion at an angle φ to a reference vector, the reference vector rotating with angular frequency ω_s. Thus, for the general ion,

$$\omega = \omega_s + \dot{\varphi} \qquad \text{.....(2.02)}$$

The equation of motion of the general ion vector with respect to the reference vector is

$$\frac{d}{dt}\left(\frac{E_s}{\omega_s^2 K}\frac{d\varphi}{dt}\right) + \frac{eV}{2\pi}\sin\varphi = \frac{eV}{2\pi}\sin\varphi_s \quad .....(2.03)$$

This represents an oscillation in the coordinate φ about the equilibrium value φ_s. The equation (2.03) is analogous to the equation for a pendulum under gravity and a constant torque. A large enough initial value of $\dot{\varphi}$ will bring the pendulum to the point of instability where it is about to swing right on over. This critical point for the pendulum corresponds to the critical point for orbital phase instability in this case. By integrating (2.03) once, we obtain

$$\dot{\varphi}^2 = \dot{\varphi}_o^2 + \frac{eVK\omega_s^2}{\pi E_s}\left[\cos\varphi - \cos\varphi_o + (\varphi - \varphi_o)\sin\varphi_s\right] \quad ...(2.04)$$

where φ_o = initial value of phase

$\dot{\varphi}_o$ = initial value of $\frac{d\varphi}{dt}$

To find the value of $(\dot{\varphi}_o)_{max}$ required to bring the phase to the brink of instability on the first positive excursion, put $\dot{\varphi} = 0$ when $\varphi = \pi - \varphi_s$. Then,

$$(\dot{\varphi}_o)^2_{max} = \frac{eVK\omega_s^2}{\pi E_s}\left[\cos\varphi_o + \cos\varphi_s - (\pi - \varphi_s - \varphi_o)\sin\varphi_s\right] \quad ..(2.05)$$

$$= \frac{eVK\omega_s^2}{\pi E_s} F_1(\varphi_o, \varphi_s) \quad .....(2.06)$$

The fact that $\dot{\varphi}_o$ occurs as a square means that the point of instability is reached independently of the sign of $\dot{\varphi}_o$ (zero damping). Therefore the maximum initial discrepancy between the ion rotation frequency and ω_s for orbital stability is $\pm\dot{\varphi}_{o_{max}}$, or the maximum range of $\dot{\varphi}_o$ over which capture of the ion into a phase stable orbit is

possible is

$$\Delta\omega_s = 2(\dot{\varphi}_o)_{max}$$

This requires correction for the factor that, for some values of $\dot{\varphi}_o$, the energy change (and radius change) of the orbit on the first negative excursion of its phase oscillation about the equilibrium orbit may be sufficient for the ion energy to pass through zero (for the orbit to contract to zero radius) if the equilibrium orbit (the energy reference for the oscillation) has not expanded fast enough. That is, at small radii the negative energy excursion with respect to the equilibrium orbit may exceed the energy of the equilibrium orbit. To include this possibility the factor 2 is replaced by $(1-\lambda)$, where λ is a function of φ_s and φ_o and can have values in the range -1 to +1. λ is not symmetrical about zero; hence the allowed $\dot{\varphi}_o$ about ω_o is now not independent of sign.

$$\Delta\omega_{acc} = (1-\lambda)(\dot{\varphi}_o)_{max}$$

$$= (1-\lambda)\left[\frac{eVK\omega_s^2}{\pi E_s}\right]^{\frac{1}{2}} \left[F_1(\varphi_o\varphi_s)\right]^{\frac{1}{2}}$$

$$= 2L(\varphi_o\varphi_s)\left[\frac{eVK\omega_s^2}{\pi E_s}\right]^{\frac{1}{2}} \qquad \text{.....(2.07)}$$

where

$$L(\varphi_o\varphi_s) \equiv \tfrac{1}{2}(1-\lambda)\left[F_1(\varphi_o\varphi_s)\right]^{\frac{1}{2}} \qquad \text{.....(2.08)}$$

Bohm and Foldy show that it is reasonable to assume that all ions start being accelerated at the center with a phase $\varphi_o = \frac{\pi}{2}$, in which case, writing $\sin\varphi_s = \rho$, we have

$$\Delta\omega_{acc} = 2L(\rho)\left[\frac{eVK\omega_s^2}{E_s}\right]^{\frac{1}{2}} \qquad \text{.....(2.09)}$$

The values of $L(\rho)$ against the variable ρ have been calculated[2],[3] and Henrich, Sewell, and Vale give its optimum value as about 0.49, corresponding to a φ_s about 30°. Using this value, and the following constants for the McGill cyclotron:

eV = 20,000 electron volts maximum energy gain per turn.

K Assuming the value at 5 inches radius is approximately constant over the central region,

= 2.18 (D.W. Hone)

φ_s Near the center this is the resonance angular frequency for protons in a magnetic field of 16,300 gauss.

= 1.57×10^8 rad/s

E_s For the total energy of the ion near the center we may use the rest energy of the proton

= 9.38×10^8 electron volts.

we have, from (2.09):

$$\Delta\omega_{acc} = 2(0.49)\ \frac{20 \times 10^3 \times 2.18 \times (1.57 \times 10^8)^2}{\pi \times 9.38 \times 10^8}$$

$$= 0.59 \times 10^6 \text{ rad/s}$$

The acceptance time is approximately

$$\Delta t_{acc} = \frac{\Delta\omega}{d\omega/dt}$$

From the static curve of oscillator frequency vs. angular position of the rotating condenser[1] and a modulation frequency of 200 cps we obtain the value for $\frac{d\omega}{dt}$ at 25.0 Mc/s of 3.32×10^{10} rad/s^2. Hence,

$$\Delta t_{acc} = \frac{0.59 \times 10^6}{3.32 \times 10^{10}}$$

$$= 18\ \mu\text{sec.}$$

This is a maximum value, for the present magnetic field, accelerating

voltage of 10 Kv, and rate of frequency sweep at the center, since the optimum value of L(ρ) was used.

The manner in which the capture efficiency is predicted to vary with accelerating voltage, modulation frequency, and other factors, is roughly confirmed by experiment(2),(3),(4) but experiment also indicates that ions released at the center over a much longer period than the above "acceptance time" are accelerated to high energies. Henrich, Sewell, and Vale, working with the 184-inch cyclotron at Berkeley, pulsed the ion source (arc type) for 2 μsec at a variable point on the f-m cycle and measured the current collected by a probe at 75 inches radius for a number of positions of the ion pulse. The curve they obtained is reproduced in figure 2. For the operating conditions under which the experiment was performed, the acceptance time calculated from the above equation was 29 μsec. If we interpret the curve as giving the relative probability of full acceleration of an ion if that ion is released at a given instantaneous frequency point in the f-m cycle, it will be seen that this relative probability is significant over a time of about 100 μsec, with a fairly sharp maximum after about 60 μsec. Henrich, Sewell, and Vale interpret the last 40 μsec of this time as corresponding to the acceptance time, and the first 60 μsec as being the time for which an ion persists in the central region after formation by the arc.

It seems reasonable to expect the shape of such a curve to be very much a function of the type of ion source used, the r-f Dee voltage, the steady Dee bias voltage, and the shape of the magnetic field at the center. Hence, although the curve indicates that a negligible increase in ion current should be expected from an ion source pulse longer than a certain optimum length, it cannot be relied upon to give more than an order of magnitude for what that optimum pulse length is

likely to be in the case of the McGill cyclotron. Since the apparatus for making similar measurements for the McGill cyclotron is not sufficiently complete at this time to give an accurate set of results, we shall assume for working purposes that the optimum length of ion source pulse is likely to be in the same ratio to the theoretical acceptance time. Since the optimum pulse length of the 184-inch cyclotron is 100 μsec, compared to the theoretical acceptance time of 29 μsec, we shall assume that the optimum ion source pulse length for the McGill cyclotron is likely to be of the order of $\frac{100}{29} \times 18 = 62$ μsec.

2. Precision:

Since the timing of the ion pulse is to occur with respect to an instantaneous frequency ω_o, we shall speak of ion pulse length and jitter in terms of the instantaneous frequency of the frequency-modulated accelerating voltage. The range of frequencies for acceptance of ions into phase-stable orbits was calculated from (2.09) as

$$\Delta\omega_{acc} = 0.59 \times 10^6 \text{ rad/s}$$

and acceptance bandwidth

$$\frac{\Delta\omega_{acc}}{\omega_o} = \frac{0.59 \times 10^6}{1.57 \times 10^8} = 0.0038$$

under optimum conditions.

In practice, the required relation between r-f Dee voltage and $\frac{d\omega}{dt}$ is not likely to be preserved throughout the acceleration sweep. The way in which $\frac{d\omega}{dt}$ varies with time, fixed by the design of the rotating condenser, determines an amplitude vs time curve for the r-f Dee voltage which, in general, it is not possible to follow exactly. The adjustment is complicated by factors such as (1) the amplitude of

the voltage on the Dee varies over the modulation cycle owing to the wide frequency range of the oscillator, (2) the average amplitude of Dee voltage may vary from time to time owing to changes in ion loading, (3) the distribution of voltage amplitude across the Dee mouth is a function of frequency, (4) static observations of these quantities may not agree exactly with their dynamic variations when the oscillator is being frequency-modulated.

A more exact adjustment might be feasible if the oscillator under pulsed operation proves amenable to amplitude modulation by an arbitrary waveform. In the meantime, the above variations in accelerating voltage mean that φ_s is bound to vary over the acceleration sweep and thus, as pointed out near the beginning of the chapter, the theoretical acceptance time considered in terms of ions reaching the target radius will be less than the value calculated above. It should not be unreasonable to assume that under some conditions of investigation the effective acceptance bandwidth may be, say, 30% lower than optimum, or practical minimum $\Delta\omega'_{acc} = 0.39 \times 10^6$ rad/s

$$\frac{\Delta\omega'_{acc}}{\omega_o} = 0.0025$$

To place the optimum pulse length properly with respect to this range of frequencies and, of more importance, to allow the carrying out of measurements on acceptance probability vs ion release time, require that the jitter in the triggering point be not more than, as a reasonable compromise, $\pm 10\%$ of the acceptance time. The required triggering accuracy will be, then, at the central ion resonance frequency 25.0 Mc/s,

$$\pm\ 0.039 \times 10^6 \text{ rad/s}$$

$$\text{or } \pm\ 0.0062 \text{ Mc/s}$$

$$\text{or } \pm\ 0.025\%$$

$$\text{or } \pm\ 1.2\ \mu\text{sec.}$$

It is observable that, owing to mechanical vibrations and machining inaccuracies, the relation between the mechanical motion of the rotating condenser and the frequency of the oscillator is not exact enough nor constant enough to provide this required precision. Hence the synchronizing of the ion source pulse to the f-m cycle can only be done electronically from the sweeping radio-frequency signal. The circuits for doing this are discussed in Chapters III and IV.

3. Regarding a minimal pulse length.

It is naturally relevant to the preceding discussion to consider why the ion source should be pulsed for the shortest possible time, rather than run continuously or be pulsed for a length of time sufficient to include all possible indeterminacies. The main factors involved in this question are listed below:

(i) Collisions. Since they are charged particles, the out-of-phase ions will have a much higher probability of being found in the orbital region of the vacuum chamber than gas molecules, particularly in the central region where the energy of the in-phase ions is low and the effect of collision is most serious. Hence, despite the fact that the number of ions in the chamber is exceedingly small compared to the number of gas molecules, the effect of excess ions in impeding the beam may be comparable. Richardson, Wright, Lofgren, and Peters, in their preliminary trials on the frequency-modulated 37-inch cyclotron[4], found that applying to the Dee a d.c. bias of 1 or 2 Kv (to sweep out drifting ions) increased the beam current by a factor of 10 at low accelerating voltages (3 Kv), had less effect at higher voltages. This result does not necessarily show the magnitude of the collision effects, however, since the action of the Dee bias is not simple, nor completely understood.

The effect of an electric field perpendicular to a strong magnetic field is to cause the orbit of a charged particle to migrate in a direction perpendicular to both fields. Consequently, we conclude that the Dee bias reduces collisions primarily by spreading out the distribution of low energy ions into a sheet parallel to the Dee mouth. Any actual removal of these ions must be effected by the vertical inhomogeneity of the electric field. In addition, part of the increase in beam current with Dee bias may come from the effect of the Dee bias on the pick-up of ions at the center. Experiments with the McGill cyclotron seem to indicate that the effect of Dee bias on the ion source is important. We can only conclude that (1) the Dee bias is probably not a complete cure for surplus ions, hence the release of ions at other times than during the acceptance time should be avoided, but that (2) there is not sufficient evidence as yet to indicate that the effect of collisions between in-phase and out-of-phase ions is serious enough to require a minimal pulse length.

(ii) Oscillator loading. Richardson, et al., remark that residual circulating ions draw energy from the oscillator, lowering the effective Q of the system and thus reducing the voltage which the oscillator is able to develop on the Dee. There is no information on the magnitude of this effect, which is very much smaller than the loading from motion of charged particles between the outside upper and lower surfaces of the Dee and the vacuum chamber wall. (The reduction of the latter is the primary purpose of the Dee bias).

(iii) Ion source cooling. Depending on the type of ion source used, it is possible that the length of pulse applied may make the difference between having to water cool the source and not.

(iv) Ion source deterioration. The life of some parts of

the ion source may be limited by deterioration under ion bombardment. Richardson, et al., found that under continuous operation the filament (100 mil. tungsten) of their arc type source lasted about 60 hours; under pulsed operation, over ten times as long.

It will be seen from the foregoing that, while it is desirable to pulse the ion source, there is nothing to indicate that the length of the pulse above a certain value is likely to prove critical in practice. This has been roughly confirmed in the operation of the McGill cyclotron. The consideration remains that a certain precision in ion pulse length and placing is required for experiments toward the understanding of the above effects.

CHAPTER III

THE PLACING OF A PULSE WITH RESPECT TO THE INSTANTANEOUS FREQUENCY OF THE CYCLOTRON SWEEPING-FREQUENCY SIGNAL.

1. Response of a resonant circuit to the f-m signal from the Cyclotron Oscillator.

In order to relate an event to the instantaneous frequency of the f-m signal it is necessary to introduce some kind of frequency selective device which will respond as the frequency passes through a certain value. The response of an electrical network as a function of frequency is normally expressed as a "network function" or "transfer characteristic", $\psi(\omega)$; $\psi(\omega)$ is a complex function giving the amplitude and phase of the network response to a steady-state excitation of constant angular frequency ω. If the excitation is applied suddenly (e.g., amplitude modulated by the unit step function), a finite time is required for $\psi(\omega)$ to attain its steady-state value. Where the network is a simple series resonant circuit, this finite time (the "build-up" time of the oscillations) is proportional to the Q of the circuit - the time constant of the amplitude of response is $\frac{2Q}{\omega_r}$. The same time constant governs the decay of the response after the sudden termination of the excitation. It might be expected that, owing to such transient effects, the response of a resonant circuit of high Q to a sweeping-frequency excitation (such as from the cyclotron oscillator), would be modified from that given directly by $\psi(\omega)$. The mathematical treatment of this problem is reviewed in Appendix A. Here we shall summarize the results as they apply to the synchronization of pulses with the cyclotron r-f accelerating voltage.

The shape of the response in dimensionless coordinates of the simple resonant circuit to a linearly sweeping frequency excitation is

determined by a parameter

$$\alpha = \frac{\delta}{\left(2\frac{d\omega}{dt}\right)^{\frac{1}{2}}}$$

where δ is the "logarithmic decrement" of the response[9]. In terms of Q ($Q = \omega/2\delta$),

$$\alpha = \frac{\omega}{2Q\left(2\frac{d\omega}{dt}\right)^{\frac{1}{2}}}$$

For the McGill cyclotron r-f system, at a modulating frequency of 200 cps, at the instantaneous frequency 25.0 Mc/s (the ion source triggering point):

$$\hat{\omega} = 157 \times 10^6 \text{ rad/s}$$
$$\frac{d\hat{\omega}}{dt} = 3.32 \times 10^{10} \text{ rad/s}^2$$

giving

$$Q\alpha = \frac{157 \times 10^6}{2(6.64 \times 10^{10})^{\frac{1}{2}}} = 304$$

The distortion of the response from the steady-state curve begins to be observable when $\alpha = 3.5$, where the maximum deviation of the current amplitude from the steady-state curve is 2%, due largely to a deviation in the quadrature component of about 4%[9]. In the case of the McGill cyclotron, this value of α occurs for a circuit Q of $\frac{304}{3.5} = 87$. This means that f-m distortion will be almost always present in resonant circuits excited by the cyclotron r-f signal. The character of the distortion is illustrated by fig. 13(a), which is a photograph of the response to the cyclotron signal of a resonant circuit with a Q of about 1200 (a quarter-wave coaxial transmission line). The response rises smoothly to a maximum, then decays in a series of beats. The beats are generated by the interference between the ringing natural frequency of the resonant circuit and the changing frequency of the excitation. Fig. 14 is a rough comparison of this response (culled from

curves plotted for other values of α in ref.(9,10) with the calculated steady-state resonance curve, showing a 40% loss in amplitude, a displacement of the maximum point in the direction of the frequency sweep of about twice the steady-state bandwidth, and considerable spreading out of the response along the frequency axis. It is obvious that these effects must be taken into account in any attempt at an accurate measurement of the instantaneous frequency at which a given event occurs.

The theory shows that the amplitude continues to increase and the rise time of the response to decrease as the Q of the resonant circuit is improved, but more and more slowly until, for a resonant circuit of infinite Q (zero losses), the response is still finite - at the value $i = \frac{\pi^{\frac{1}{2}} E}{\left(2\frac{d\omega}{dt}\right)^{\frac{1}{2}} L}$ where L is the inductance in the simple series resonant circuit, and E is the amplitude of the excitation. For this extreme condition the leading edge of the response to the cyclotron r-f signal plotted against instantaneous frequency will have, theoretically, a rate of rise corresponding to the steady-state curve for a circuit Q of about 350. That is, no matter how selective a tuned circuit or tuned amplifier one builds to obtain a high precision in triggering point, it seems that this figure is an upper limit to its effective bandwidth for sweeping-frequency signals. For this reason, the triggering unit for the ion source (described in the next chapter) was built around a passive network rather than attempting to gain the last iota of rise time (and distortion) from a highly selective (st.-st.*) tuned r-f amplifier or superheterodyne receiver circuit. The presence of f-m distortion in the band-pass filter used is plainly evident in the photograph of fig. 3(a), in the difference between the responses to the increasing-frequency sweep and the decreasing-frequency sweep. The Q's of the components in the

* steady-state

filter are about 250. The question of evaluating the distortion and correcting for it has not yet arisen in practice, since the trigger point is made variable in frequency and is adjusted to give a maximum of ion current at the target without regard to the actual instantaneous frequency at which the ion source is pulsed.

Note; The above discussion is entirely based on the response of a simple series resonant circuit. It is anticipated that there are endless possibilities in the design of networks specifically for sweeping-frequency use, taking advantage of the continuously changing phase of the excitation, which will be worked out as this type of circuit analysis becomes more familiar. Because of the partly empirical design of the r-f filters described in the next chapter it is very likely that some use has been made of these factors but the extent of their contribution is not known.

2. Relation between the required trigger circuit bandwidth and the ion acceptance bandwidth.

From Chapter II, we have

$$\Delta\omega_{acc} = 2L(\rho)\left[\frac{EVK\,\omega_s^2}{\pi E_s}\right]^{\frac{1}{2}} \qquad \text{.....(2.09)}$$

and $$-\frac{1}{\omega_s^2}\frac{d\omega_s}{dt} = \frac{KeV\sin\varphi_s}{2\pi E_s} \qquad \text{.....(2.01)}$$

$$= \frac{KeV\,\rho}{2\pi E_s} \qquad [\rho = \sin\varphi_s]$$

Combining these to eliminate the factor $\frac{KeV}{\pi E_s}$, we have

$$\Delta\omega_{acc} = \frac{2L(\rho)}{\rho^{\frac{1}{2}}}\left[2\,\frac{-d\omega_s}{dt}\right]^{\frac{1}{2}} \qquad \text{.....(3.01)}$$

$[\omega$ decreasing$]$

For the electrical circuit case, write $\frac{1}{Q} = \frac{\Delta\omega_t}{\omega_o}$, where $\Delta\omega_t$ is the "slow-frequency sweep" bandwidth of the trigger circuit required for a certain precision in placing the ion source pulse with respect to the instantaneous frequency of the accelerating voltage. Then the response parameter α determining how nearly this bandwidth can be realized is

$$\alpha = \frac{\Delta\omega_t}{2\left\{2 - \frac{d\omega}{dt}\right\}^{\frac{1}{2}}} \qquad \ldots\ldots\ldots\ldots\ldots\ldots\ldots\ldots\ldots\ldots (3.02)$$

Substituting for $(-2\frac{d\omega}{dt})^{\frac{1}{2}}$ from (3.01),

$$\alpha = \frac{\Delta\omega_t}{\Delta\omega_{acc}} \quad \frac{L(\rho)}{\rho^{\frac{1}{2}}} \qquad \ldots\ldots\ldots\ldots\ldots\ldots\ldots\ldots\ldots\ldots (3.03)$$

This means to say that the limitation on the realizability of $\Delta\omega_t$ is a function only of the desired accuracy with respect to the theoretical acceptance time, and the ion capture efficiency function $\frac{L(\rho)}{\rho^{\frac{1}{2}}}$, and is independent of the particular cyclotron or operating conditions thereof, except insofar as the range of orbital phase-stability differs from the ideal. There is apparent a close analogy between the response parameter α for the resonant circuit, and what might be regarded as a response parameter for ions to pick-up by the accelerating field into stable orbits $\frac{L(\rho)}{\rho^{\frac{1}{2}}}$. It is suggested that a "sweeping-frequency" approach to the question of the phase-stability of ion orbits might exhibit the meaning of this analogy more explicitly.

CHAPTER IV

THE MCGILL ION SOURCE SYNCHRONIZING SYSTEM

1. The R-F Signal Source.

The r-f signal for the synchronizing circuits is tapped off the plate coupling loop of the oscillator near the grounded end by a sliding silver-to-silver contact which allows adjustment of the amplitude between 1-40 volts. This is set to give about a five volt signal at the control room end of a 52 ohm cable. The treatment of the signal in the control room is shown in the block diagram, fig. 4.

A switch at the input of the synchronizing unit selects between the r-f signal from the cyclotron room, and a locally generated signal from a reactance-tube modulated oscillator for testing purposes. The signal then passes through a limiter (6AG7) which smooths out the variations in amplitude due to incidental 200 cps amplitude modulation of the oscillator, changes in oscillator plate voltage, vacuum conditions in the tank, and difference between the alternative sources, in addition to clipping off any transient pulses so that the ion source is less likely to be triggered by occasional sparks and breakdowns.

2. Discrimination between Increasing and Decreasing Frequency Sweeps.

Now, if this signal were simply put into a tuned amplifier two pulses would appear, roughly the shape of resonance curves, one on the increasing-frequency part and one on the decreasing-frequency part of the modulation cycle. It is only near 25 Mc on the decreasing-frequency part that a synchronizing pulse is desired; hence it is necessary to discriminate between the two pulses - while still allowing for varying the trigger point over a range of frequencies. The Berkeley cyclotron group accomplished this by taking the roughly sinusoidal waveform

from the output of a frequency discriminator, shifting it 90° in phase, and squaring it up into a gating pulse to let through only the pulses from the desired quarter of the modulation cycle. The Rochester cyclotron used a gating circuit triggered from another point in the f-m cycle. We have used a circuit which is more direct, and probably more flexible for use in other apparatus or under pulsed oscillator operation since it does not make use of other parts of the cycle to select the correct pulse.

Instead of a simple tuned receiver, the signal is put through a band pass filter with the low-frequency side of its transmission characteristic very much steeper than the high-frequency side, as shown in fig. 3(c). The rectified envelope of the output voltage of the filter, generated as the frequency sweeps through its transmission region, has a steeply rising or steeply falling discontinuity corresponding to the steep side of the band-pass characteristic according to whether the frequency is changing with time in an increasing or a decreasing direction, and comparatively slower falling and rising slopes generated by the other (the high-frequency) side of the characteristic. After "differentiation" of the rectified envelopes the above slopes appear as the leading edges of pulses, positive and negative as the slopes are rising or falling with time, and with amplitudes dependent on their steepness. Thus, as arranged here, the low-frequency side of the filter characteristic generates a negative pulse at the signal grid of the amplifier tube (6AC7) following the differentiating network, as the frequency sweeps by in the decreasing direction. This is distinct from the positive pulse resulting from the increasing-frequency sweep, and considerably larger in amplitude than the negative pulse generated by the high-frequency edge of the filter from the increasing-frequency sweep.

3. The Band-pass Filter.

The first filter designed for this purpose, which has been in use for some months, is of the configuration[27] shown in fig. 5(a). The link coupling between the end sections, an empirical addition, apparently serves two purposes: (1), improves the constancy of amplitude and phase shift across the pass band, (2), counteracts tracking errors between the end sections as the filter is tuned. While this filter has the advantages of a large difference between the slopes of the two sides of the band-pass characteristic, and a convenient configuration for tuning by ganged capacitors, it has the disadvantage of operating at a rather low driving point impedance due to the series-tuned elements in the shunt arms and the importance of stray capacitances across the terminations at these frequencies. This low driving point impedance means that the r.f. amplifier feeding the filter cannot develop a high gain.

This condition is rectified in the filter shown in fig. 5(b) which is being incorporated along with other modifications in a new synchronizing unit. The tuning capacitors across the end sections absorb the circuit strays, and the impedance looking into the filter rises to very high value in the pass band. The parallel L and C in the shunt arm on the output side form not, as might appear, a resonant element, but a large inductance, contributing a transmission peak at a frequency just above the rejection peak from the parallel resonance of the series arm. The capacitance serves to keep this element on the inductive side of resonance as the filter is tuned. If the tuning range is less than 1 Mc/s as for the ion source trigger (the same circuit is used to trigger the monitoring oscilloscope over a much wider range) this capacitor may be left fixed. The tuning of the filter elements and the coupling between them were adjusted experimentally with a

sweeping-frequency generator and oscilloscope. The required difference in the slopes of the edges of the filter characteristic was made less extreme by the use of the non-linear differentiating circuit described below.

4. The Differentiating Circuit.

A simple linear network (of C and constant R) would entail considerable attenuation of the desired pulse, say about 1/10, to accomplish the necessary discrimination between the two slopes from the filter characteristic of fig. 3(c). A much higher efficiency is obtained from the circuit at the grid of the 6AC7 amplifier tube shown in the detailed circuit diagram fig. 6. An approximate mathematical treatment of the circuit is given in Appendix B. The "circuit" consists only of returning the 6AC7 to the anode voltage supply through a resistor such that certain approximate relations hold between the grid current, the coupling capacitance, and the rate of rise of the desired pulse. The input resistance of the 6AC7 serves as the resistance of the differentiating network and is low when grid current is flowing, increasing logarithmically as the grid current is decreased. Thus a negative sloping pulse sufficiently steep that the current through the capacitance is slightly greater than the current flowing from the anode voltage supply encounters a high input resistance and suffers very little attenuation as it drives the grid negative, generating a large positive pulse at the anode to trigger one or more thyratrons in the following stages. The less steeply falling pulse encounters a lower value of R and is attenuated in exaggerated proportion. A cathode follower detector circuit is used so that this low resistance does not affect the Q of the filter elements. Longer time-constant overshoots mostly due to the drawing of additional grid current by the positive pulses are practically eliminated from the

amplifier output by a short time constant in the screen grid supply.

The end result is shown in fig. 3(d). The small pulse on the left is all that remains of the effect of the increasing-frequency signal on the filter. The leading edge of the positive pulse on the right (amplitude 80V) represents the amplified low-frequency side of the filter characteristic. As noted on fig. 3(c) the frequency width of this side of the characteristic is 0.12 Mc/s. A small part of the beginning of this edge is lost at the amplifier grid as grid current ceases and the grid voltage begins to go negative, and part at the end of the edge is lost as the grid is driven towards cutoff (the screen grid voltage is made low to obtain a short grid base). Hence the leading edge of the pulse from the amplifier represents a section (not more than 3/4) of this filter edge, and is therefore rising at a rate of approximately

$$\frac{80}{0.12} \times \frac{4}{3} = 890 \text{ volts/Mc}$$

The allowed error in triggering frequency worked out in Chapter II was $\pm$ 0.0062 Mc/s. This represents a voltage range on the leading edge of the above pulse of $\pm$ 5.5. volts, or 13% of the total amplitude of the pulse. Even long term variations in the triggering point of the type 2050 thyratron due to heater-voltage variations and aging of the tube will be less than 1/10 of this voltage range. The largest sources of error will be (1) noise arriving with the r-f signal, (2) change in the shape of the beginning of the pulse as the grid current characteristic of the 6AC7 changes with age, (3) changes in the total amplitude of the pulse from aging of tubes and variations in supply voltages. It is estimated that none of these errors can exceed the allowed margin in hour-to-hour operation. The jitter from cycle to cycle should be less than 10% of the allowed margin. The latter figure is useful in the

monitoring of the pulses, giving less than 0.2 μ sec jitter between the ion source pulse, for example, and the oscilloscope time base triggered just before it.

5. The Pulse Gating System.

For some experiments the pulses of high energy protons from the cyclotron are required to be intermittent. For the exposure of nuclear emulsions, for example, a single pulse may be desired, and for other experiments perhaps pulses at arbitrary intervals. It was assumed that it would be sufficient for most of these applications to pulse the ion source in this way. It has since become apparent that stray ions are accelerated on every modulation cycle as long as the r-f accelerating voltage is applied to the Dee whether the ion source is pulsed or not, and that the only satisfactory procedure for such experiments is to pulse the oscillator. Hence, while the following gating system (described in more detail in Appendix C) may prove of limited usefulness in the ion source pulsing system, it is proposed to apply it unchanged to controlling the pulsing of the r-f oscillator.

Four types of pulsing are allowed for:

(1) Continuous; a pulse at the required instantaneous frequency point once every modulation cycle.

(2) Intermittent; pulses at the proper frequency point at arbitrary regular intervals.

(3) Single; one pulse at the first proper frequency point after pushing a button.

(4) External; provision for synchronizing intermittent or single pulses with a particular experimental apparatus.

Referring to the circuit diagram (fig. 7), the operation is

built around the fact that, with the values of anode and cathode resistors used here, the discharge of the thyratron T_1 is not self-extinguishing. After T_1 has been triggered, discharging C_1 through the cathode resistor to form the ion source trigger pulse, it continues to conduct (not heavily, because of the large voltage drop across the charging resistor R_1) but sufficiently to keep C_1 discharged. The continued positive pulses on the control grid cannot cause another pulse forming discharge until the ionization in T_1 is extinguished and C_1 is allowed to charge up again. The extinction is brought about by the thyratron T_2, whose sudden conduction applies a negative pulse to the anode of T_1, at the same time that a large negative square pulse is applied to the second control grid of T_1. The pulse on the second grid assists in extinguishing the ionization and at the same time prevents the thyratron from being triggered by a positive pulse on the first control grid until the condenser C_1 is fully charged. This manner of using a two-grid thyratron was introduced by Mr. P.B. Troup.

In this way, the trigger generating thyratron T_1 is normally in the discharged condition and can generate a pulse only after "priming" by the control thyratron T_2. The "pulsing type" switch governs whether:

(1) For continuous pulsing T_2 is triggered on every cycle, from the same pulse which triggers T_1.

(2) Intermittent: T_2 becomes a relaxation oscillator, priming T_1 at its own repetition rate.

(3) Single: T_2 is triggered each time the "single pulse" button is pushed.

(4) External: T_2 is triggered from an external source.

The cathode of the trigger generating thyratron is connected to a 52 ohm line to the cyclotron room through a relay. The relay is energized by a "Pulse Ion Source" button on the main cyclotron control panel. This allows the setting up and testing of the trigger point and mode of pulsing before introducing ions to the vacuum chamber (other than

the stray ions already there from the residual gas). In the cyclotron room the trigger pulse sets off the ion source pulse generator (designed by Mr. P.M. Milner) which applies a large square pulse (of the order of 100 volts and 100 amperes) 2 to 150 μ sec in length to the ion source. The length of the pulse is determined by a "phantastron" circuit controlled by a variable potential from the pulse synchronizing unit.

CHAPTER V

OTHER SYNCHRONIZED ELEMENTS

1. Deflector.

It should be clear from Chapters III and IV that the synchronizing system described for the ion source is not capable of generating a trigger pulse with an indeterminacy in the frequency point of less than one r-f cycle, which is the precision required for the most efficient deflection of the beam[5]. This, however, is a required precision with respect to the phase of an r-f cycle within a small range of frequency, rather than with respect to such an exact instantaneous frequency. Hence it has been decided in consultation with Mr. D.W. Hone that the most promising arrangement is a combination of the above type of trigger generator (Chapt. IV) to choose the instantaneous frequency point, with another circuit to synchronize with the r-f phase within a small range about this point. The latter circuit is an intimate concern of the deflector problem and will not be discussed here.

2. R-F Oscillator Pulse.

Since the synchronizing methods described above are dependent on the r-f signal, they are plainly unsuited to the synchronizing of the oscillator pulse. Since the oscillator pulse should be just longer than the duty cycle, it should be synchronized with a fair accuracy to the position of the rotating condenser (say, within 0.5 Mc/s). A mechanical method immediately suggests itself, but, in view of the inaccessibility of the rotating condenser shaft, the following method appears more promising in precision and convenience.

A fixed-frequency "control" oscillator of low power is loosely

coupled to the resonant Dee system. A sudden dip in its amplitude of oscillation occurs as the rotating condenser sweeps the Dee system through resonance. This sudden change in amplitude can be amplified to form the required trigger pulse. It is anticipated that protection of the control oscillator from overload when the main oscillator starts will not be too difficult. If the control oscillator is not tuned to the highest resonant frequency of the Dee system, there will be two pulses generated in the same way as discussed in Chapter IV and it will again be necessary to discriminate between them. This may be done by making use of the behaviour of high Q tuned circuits with sweeping frequency signals as described in Chapter III and Appendix A. Since the resonant circuit of the control oscillator will have a very high (theoretically infinite) Q, there should be an appreciable displacement of the point of maximum response in the direction of the frequency sweep. A detector circuit tuned slightly to one side of the control oscillator frequency should then show a differential effect.

Preliminary experiments on this method initiated very recently by Mr. J.D. Keys and Mr. W.H. Henry have shown it to be practicable without working out further details.

3. Dee Bias.

The effect of the Dee bias in displacing the center of rotation of orbits along a line parallel to the Dee mouth, acting in opposition to the focussing effect of the magnetic field gradient, may encourage radial oscillations of the orbits to the point of instability. Consequently, Professor Foster has suggested that it may prove advantageous to remove the bias from the Dee during the acceleration sweep. The pulse to

accomplish this would be synchronized from the ion source trigger pulse directly or after a short delay, depending on the effect of the Dee bias on the pick-up of ions, which is an effect still under investigation.

CHAPTER VI

THE CYCLOTRON MONITORING SYSTEM

1. The Particular Problems.

The problems peculiar to the monitoring of the cyclotron arise from three causes:

(i) Remote Control Operation. This necessitates many leads from 120 to 200 feet in length between the control room and units in the cyclotron room.

(ii) The short pulses of high peak power used for ion source (up to 20 kilowatts) and deflector (greater than 16 megawatts) as contrasted with the small signals from experimental apparatus and low power monitor points.

(iii) Wide Frequency Range. Some signals to be displayed may comprise high-frequency pulse components mixed with a low modulation-frequency component.

Considering the last first, it will be apparent from the monitor displays described in the next chapter that some pulses may have a rise time as short as 0.1 μsec; if these are to be observed the oscilloscope amplifiers must have a frequency response up to 2.5 or 3 Mc/s. Other signals, such as the Dee voltage amplitude envelope, may show a fundamental component of the modulation frequency (as low as 100 cps). This particular signal may have a sharp discontinuity superimposed, in consequence of a periodic breakdown or a sharply resonant absorption. If we suppose the discontinuity to be, for example, a "notch" 1 μsec in length which is to be displayed in its correct position relative to the modulation cycle then the signal circuits must have equal delay times for the 100 cps and the 0.5 Mc/s components[6]. This imposes rather stringent restrictions

on the allowable phase distortion in the amplifier.

Most of the signals required for monitoring originate in the cyclotron room and must be transmitted without distortion to the control room through the long leads of (i). The cable used for the signal is a 300 ohm twin-core shielded cable with polythene insulation. A length of 120 feet of this cable is a quarter wavelength at about 1.2 Mc/s. Since it is required to transmit higher frequencies than this, the cable must be correctly terminated, and fed by cathode follower amplifiers.

It is the combination of (i) and (ii) that causes the most trouble in obtaining clear and unambiguous displays. Owing to the many different units operated from the control desk, all having some connection, capacitive or direct (inductive) to the cyclotron frame, there are many more or less independent paths between the control room "ground" and the cyclotron room "ground". These points may usually be regarded as the same for a.c. and d.c. power purposes, but for high frequency pulses the long leads mean that they must be regarded as separated, by a number of parallel paths of differing impedance. If e_G is the effective voltage generator in the outer conductor of the cable due to a circulating earth current then, looking from the receiving end, e_G appears in series with the monitor signal voltage generator. The most serious of such interference voltages arise between units in the cyclotron room where the heavy current pulses of (ii) circulate, as, for example, between the "ground" points in the cathode follower unit to be described, the ion source pulser, and the cyclotron frame. Briefly, the problem becomes that of observing the potential difference between two points, neither of which is at ground potential. This problem forced the development of the balanced line and differential amplifier system described in the following section.

2. The Balanced Line System.

The wide frequency range required for the transmission system makes impractical the use of balanced transformer matched lines as in telephone and telegraph systems. Instead, a balanced two-core coaxial line is used, fed at the cyclotron room end by two cathode followers in push-pull, as shown in fig. 8. The interference signal is generated in both cathode followers in the same phase with respect to the shield; at the receiving end the signal from one cathode follower is inverted and added to the signal from the other in the circuit shown in fig. 9. The interference signals are cancelled out and the monitor signals add. Thus only the signal applied between the two input points appears in the output — provided that the interference signal e_G added to each input does not cause the total signal to exceed the linear range of the cathode followers and phase inverter.

A single balanced system, switchable by remote control to any one of five inputs, is used to transmit all monitor signals from the cyclotron room. There are six sections in the switch - one for each of the five balanced inputs, and one to connect only the active pair of leads to the cathode follower grids. Careful shielding in the switch is necessary to prevent stray couplings between the inputs. A hand-made follow-up motor and switch arrange for a one-to-one correspondence between the remote inputs and the monitor point switch on the control panel.

The cathode followers (fig. 8) are two 6SN7 duo-triodes, cross-connected so that one triode unit of each is in parallel with one triode unit of the other. The two triode units in parallel, with a cathode load of 700 ohms, present an effective output impedance of 150 ohms to match one half the characteristic impedance of the line, and give a gain of 0.8 . The two tubes are cross-connected so that the

balance is not likely to be affected by variations in aging between the two tubes, and so that the tubes do not have to be picked for identical characteristics. The operating grid bias is -8 volts, giving a reasonably large dynamic range. The exact matching of the line is adjusted by the variable resistors in parallel with the cathode loads, using 100 Kc/s and 1 Mc/s test signals from a square wave generator.

The signal mixing circuit (fig. 9) consists essentially of two cathode followers, T_1 and T_2, sharing a common cathode load. The signal from one side of the balanced line from the remote unit is applied directly to the grid of T_1; the signal from the other side of the line is inverted by the "gain-of-minus-one amplifier", T_3, before reaching the grid of T_2. The voltage across the cathode load is transmitted by six feet of shielded cable to the oscilloscope, mounted in another section of the control rack. The cathode follower amplifier is used extensively in these circuits because of its inherently low distortion, and because of the low effective generator impedance required to transmit the high frequencies through the long interconnections. The balance of the mixing circuit is adjusted by joining the two input terminals, applying the square wave test signals between the joined terminals and ground, and varying the input to the phase inverter for minimum signal on the oscilloscope. Complete cancellation of the highest frequency components is not possible with the mixing unit in use at present, probably because of asymmetry in the circuit wiring, but the interference signal is reduced by a factor of about 20. This is sufficient to fulfil one purpose in eliminating interference pulses, which is to prevent overloading of the oscilloscope amplifiers in the attempt to examine smaller signals occuring at other times in the modulation cycle. A much better reduction should be obtainable in the re-designed unit under construction.

A unit designed to supply a push-pull balanced signal to this system is the Dee Voltage Detector, fig. 11. The signal may equally well be applied to one side only of the balanced line, except that the maximum amplitude of signal possible in the output is halved. For an unbalanced input the interference may be minimized by arranging the terminations at the source, and at the input terminals of the remote cathode follower unit, so that the interference voltages appearing at the two cathode follower grids are equal.

The switch S, (fig. 9) in the signal channel from the frequency discriminator (see Ch. VII, 1) arranges for any pulse monitored to be displayed superimposed on the Frequency vs Time curve to show its approximate location in the modulation cycle. The photograph in fig. 13(a) shows the ion source trigger pulse displayed in this way.

3. The Oscilloscope.

The oscilloscope in use was adapted early in the setting up of the cyclotron from a design by Fitch and Titterton[7] as a useful general-purpose expedient until the monitoring needs were worked out more precisely as they arose in practice. The video amplifier has since been revised and rebuilt by the author to fit in with the system described in the previous section. A high impedance cathode follower input and a video delay line were formerly incorporated. Since the signal is supplied at a low impedance from the signal mixing circuit, the high impedance input was unnecessary; the delay line was not needed since the variable frequency triggering circuit provides an independent delay of any length. One amplifier stage was added to increase the gain to about 1000, partly to compensate for the losses in the cathode followers and long lines. The compensated attenuator network which was designed to work into the high input impedance

of the cathode follower was redesigned to a lower impedance to match the input impedance of the added amplifier stage. The mechanical construction was revised for more complete shielding and for more convenient mounting in the control rack.

In its present form, the frequency response of the video amplifier is down 0.5 db at 40 cps and 2 Mc/s. There is about 10^{o} phase shift between 100 cps and 2 Mc/s. The consequent displacement of the apparent position of a very short pulse with respect to the modulation cycle does not seriously affect the usefulness of the display, since any accurate measurement of the instantaneous frequency position of the pulse would in any case be done with a calibrating mark from a local oscillator*. The time base is a triggered time base, as opposed to a "free-running sawtooth" type, and may be triggered either from any desired point on the decreasing-frequency part of the modulation cycle, or from the video signal. The frequency triggering circuit is similar to that used for the ion source except that the thyratron is self-extinguishing. The slowest sweep displays one modulation cycle at 100 cps; the fastest sweep has a writing speed of about 1 inch/μ sec.

* Nonetheless, the deception should be eliminated in the proposed re-design of the oscilloscope unit (Ch. VIII).

CHAPTER VII

OSCILLOSCOPE DISPLAYS

1. Frequency vs. Time.

This is the most generally useful picture since it displays the frequency modulation cycle, to which all the synchronizing is related. It indicates that the frequency is changing smoothly with time in accordance with the theoretically required curve, and shows the position in frequency of any transient breakdowns. The signal is approximately sinusoidal with a fundamental component of from 100 to 400 cps., depending on operating conditions (fig. 13a).

The frequency discriminator, (fig. 10), is a conventional design[8], chosen because the many variables (coupling coefficients, resonances, and damping) allowed a closer adjustment of linearity over the wide frequency range (19 - 28.5 Mc/s). The 6AK5 limiter follows the more rugged 6AG7 limiter on the r-f input described in Chapter IV. A longer time constant is used in the grid circuit to give an amplitude smoothing action somewhat complementary to the first limiter.

The Q's of the tuned circuits are about 2 or 3, consequently there will be no observable distortion in the response to the f-m signal from the statically measured characteristic. The values of components and coupling coefficients were worked out empirically for the most part, since this is the quickest and surest design procedure at these frequencies.

2. R.F. Dee Volts vs. Time, or vs. Frequency.

It is important in obtaining the maximum accelerating efficiency from the cyclotron to maintain the correct relationship

between frequency and amplitude of the accelerating voltage over the duty cycle, as was pointed out in Chapter II. To aid in the adjustment of this relationship the detector circuit of fig. 11 was designed to exhibit the dynamic variations in oscillator voltage near the mouth of the Dee. It cannot be expected that the dynamic picture will be identical to the curve obtained by measurement of the oscillator voltage at steady-state fixed frequencies, owing to the effect of various time constants in the grid bias and power supply circuits, and owing to probable differences between transient and steady-state oscillating conditions at different frequencies. Needless to say, this picture is doubly important for pulsed operation of the oscillator. The signal is similar in character to (1) above, but is generated near the cyclotron Dee and hence must be passed undistorted through about 150 feet of cable to the control room display.

The probe shown at the upper left of fig. 11 is a heavy copper wire about three inches long mounted near one end of the Dee mouth on a Kovar seal through the upper lid of the vacuum chamber. Since the voltage picked up on the probe cannot be measured at full oscillator voltage until the vacuum chamber is closed and evacuated, a capacitive attenuator is provided to adjust the input to the high-impedance detector to about 20 volts. All leads in the input circuit have been kept as short as possible to avoid any resonance effects. A 15 megohm resistor from the probe to ground provides a leakage path for stray ions which otherwise might build up a high voltage across the input capacitor.

Under continuous (not pulsed) operation of the oscillator the display of the amplitude envelope of the Dee voltage would be meaningless unless the average value were known about which the variations in amplitude took place. Here a reference is obtained by returning the

detector to the zero input point by a short pulse once each modulation cycle. A positive pulse from the cathode of the thyratron which triggers the oscilloscope is transmitted by a 52 ohm cable to the cyclotron room where it is inverted by a pulse transformer outside the strong magnetic field and passed on as a 30-40 volt negative pulse to the grid of the cathode follower detector. A 1N34 germanium diode where the pulse enters the detector unit clips off the positive overshoot. A second 1N34 diode prevents the detector output from being driven below the quiescent (no signal) point by the large negative pulse on the grid. The 10,000 ohm resistor between the cathode and this diode improves the clamping action of the diode, since otherwise the (low) output impedance of the cathode follower is commensurable with the forward resistance of the diode, especially when the voltage across the diode is small (near the clamping point). The 50,000 ohm potentiometer is adjusted so that small negative pulses are just observable in the output when the r-f input is zero.

The detector is followed by a phase inverter to supply the push-pull signal to the balanced cathode followers, which then feed the signal through about 30 feet of 300 ohm cable to the remotely operated switching unit described in the previous chapter. The entire circuit is enclosed in a copper box which is screwed down to the vacuum chamber lid over the probe lead-through.

A typical resulting signal is shown in fig. 13(b). Two modulation cycles are visible on the trace. The oscilloscope time base is starting on alternate trigger pulses so that one r-f amplitude reference pulse is observable in the center of the picture. Amplitude modulation over the f-m cycle is plainly evident. Near the place of maximum amplitude a small dip is observable which comparison shows is successfully eliminated by the limiters so that it does not show in

the frequency vs time display of fig. 13(a). Other small pulses result from insufficient shielding in the synchronizing and monitoring unit - a condition which is eliminated in the re-designed unit shortly to be installed. The amplitude vs frequency curve is not observable on the present monitor oscilloscope since it is without a horizontal deflection amplifier to display the Frequency vs. Time curve as a base. It may be observed on a portable oscilloscope by making connections to the appropriate points in the signal mixing circuit.

The filaments of the vacuum tubes in the detector unit are heated by d.c. and the power supply transformers and rectifiers are mounted with the pulse transformer in a separate chassis well away from the strong magnetic field. In spite of these precautions the output of the unit is affected by the field so that if observations are desired while the cyclotron is in full operation, some modifications will be necessary. It is thought inadvisable to attempt magnetic shielding of the detector unit in its present position, since a large block of iron so near the pole pieces might distort the cyclotron magnetic field. Hence the modifications will probably involve mounting a germanium diode detector at the Dee voltage probe, with a d.c. connection via a low capacitance shielded lead to a pulsed amplifier or cathode follower unit similar to the above, mounted in a magnetically shielding box two or three feet away from the pole pieces. Time has not permitted the carrying out of these modifications up to the time of writing.

3. Ion Source Pulse.

This is a roughly square topped pulse 2 μ sec to 150 μ sec in length. The peak current is of the order of 50 to 200 amperes. Fig. 13(a) is a photograph of the current pulse into a cold-cathode ion

source designed by Mr. P.M. Milner. The series resistor was 1/20 ohm in the lead from the grounded side of the ion source to the pulse transformer.

In the case of the arc type ion source previously used the observation of the current pulse was complicated by the fact that the leads from the pulse transformer to the ion source also carried the ion source filament current of 300 to 400 amperes. This made the insertion of a series resistor impractical and the most satisfactory monitor point for working purposes was found to be the cathode current of the final amplifier working into the primary winding of the pulse transformer.

4. Ion Source Trigger Pulse.

This is displayed to make sure that it is present at the correct frequency point, without jitter, and set up for the required mode of pulsing the ion source, before it is connected by the "Pulse Ion Source" relay to the cable to the pulse generator in the cyclotron room.

5. Probe Current Pulse.

The observation of the peak beam current collected on a probe is important for the adjustment of the cyclotron to optimum working conditions. The pulse has an overall length of the order of the acceptance time, and a fine structure with a period corresponding to the orbit precessional frequency(3). The precessional frequency is given by

$$f_{pr} = f_o \left[1 - (1 - n)^{\frac{1}{2}}\right]$$

For the McGill cyclotron, at a radius of 36 inches,

f_o = 21.8 Mc/s and n = 0.0825, giving

$$f_{pr} = 0.9 \text{ Mc/s}$$

The integrated pulse, measured across a high resistance of 220,000 ohms is shown in the photograph 13(d). To observe the fine structure requires a much shorter time constant of the discharge path across the probe and therefore a much lower resistance. The voltage across the resistor decreases in proportion so that a pre-amplifier becomes necessary. The required pre-amplifier (gain of about 100, frequency response up to 2 Mc/s) has not been available up to the time of writing.

6. Deflector pulse.

This is an extremely short pulse (less than 0.05 μ sec) of a very high peak power (greater than 16 megawatts)[5]. Hence, as far as the oscilloscope display is concerned, it may be difficult to avoid seeing when it occurs, but the accurate observation of its shape must be left to a specialized synchroscope.

7. Other Information.

(i) Fixed frequency 1 and 5 Mc/s calibrating oscillators are incorporated in the frequency-modulated test-signal generator to generate frequency calibration markers on the display when their signals and harmonics are mixed with the f-m signal in the discriminator circuit.

(ii) The modulation frequency, or repetition rate of the f-m cycle, can be read directly from a meter on the control panel. The circuit for this meter is shown in fig. 12. A standard current pulse is

formed once per cycle by a thyratron triggered from the ion source trigger circuit (see fig. 7 and App. C). The current pulses are integrated by a network which includes the indicating meter (100 μamp full scale). The current through the meter is directly proportional to the repetition rate of the pulses and is adjusted by the bias on the diode to read 1000 cps full scale. The re-charging time of the thyratron anode circuit limits the current at higher repetition rates so that the meter cannot be overloaded. (Occasionally, gas discharges in the vacuum chamber cause large numbers of transients in the r-f signal some of which get through to the thyratron grids).

CHAPTER VIII

PROJECTED ADDITIONS

The synchronizing and monitoring arrangements for the McGill cyclotron, as described in the preceding chapters, are not complete. Indeed it could not be expected that they should be - as if a thesis on such a subject could be written as a closed book. As a contribution towards the further development of the arrangements it is proposed to list some of the improvements which have appeared desirable from the experience gained up to this time, and which may be carried out as time and labour become available.

1. Re-design of the Oscilloscope Unit to Include the following features.

(a) A 5-inch cathode ray tube with triggered time base as at present, for the close examination of pulses at any point in the acceleration sweep but with an improved video amplifier to introduce less phase shift at low frequencies. Provision should be added for calibrated time and frequency markers for the accurate measurement of pulse forms and their posttions in the f-m cycle. (It will be a problem in itself to calibrate all channels for time delays and f-m distortions). At least as high a gain as at present is desirable but without the slight microphonic effects arising from the rigid mounting of the first amplifier stage.

(b) An additional smaller (3-inch) cathode-ray tube for a permanent display of the modulation cycle and ion source pulse, with a simple synchronized sawtooth time base. This display is useful for a continuous index to the cyclotron operation in addition to whatever signal is being examined more closely on the larger display.

2. Integration of the oscillator pulse synchronizing system into the system

already described.

3. Revision of the Dee Voltage Detector as discussed in (VII, 2).

APPENDIX A

RESPONSE OF CIRCUITS TO A SWEEPING-FREQUENCY EXCITATION

This section comprises an introduction to the mathematical treatment of the sweeping-frequency phenomena discussed in Chapter III. The acceleration of ions in the synchro-cyclotron may be regarded as a response of the resonant ion orbits to a driving function (the r-f accelerating field) which is periodic with a frequency which changes with time. The synchronizing of auxiliary functions (such as the ion source pulse) to the acceleration of ions depends on the response of circuit elements to the same driving function. Hence it is important for a full understanding of the working of the synchro-cyclotron to become familiar with the nature of this driving function and its effect on responding elements.

Mathematically related problems arise in a variety of applications: in the response of a resonant system to a variable-frequency excitation[9-13], in the acceleration of rotating machinery through a critical speed[14], in the sweeping of parameters through resonance in the measurement of nuclear magnetic moments[15], in the passage of ion orbits in a synchro-cyclotron through a critical region of coupling between radial and vertical oscillation[3], and very probably in the capture of ions at the center into phase-stable orbits (III, 2).

The electrical circuit case has been receiving increasing attention in the last few years owing to the development of f-m radio transmission, and owing to an increasing use of sweeping-frequency generators in the test and design of r-f components. There have been numerous treatments of the distortion of f-m signals in electrical networks for the types of frequency modulation used for radio transmission, most of them by expansion

of the network and driving functions in finite series of steady state terms such as Fourier series, Taylor series, Legendre polynomials, etc.[16-23]. These methods are not generally suitable where the frequency deviation is large because the number of terms in the expansions becomes excessive. For example, the Fourier expansion of a f-m wave is[24]

$$E = \sin(\omega_o t + m \sin vt)$$

$$= \sum_{n=-\infty}^{\infty} J_n(m) \sin(\omega_o + nv)t \qquad \text{.....(A.01)}$$

The amplitudes of the Fourier components are determined by the Bessel functions $J_n(m)$, where m is the "modulation index", defined as

$$m = \frac{\text{frequency deviation from the mean}}{\text{modulating frequency}}$$

$$= \frac{\Delta f}{v/2\pi}$$

For the McGill cyclotron $\Delta f = 3.6$ Mc/s; for present operating conditons $\frac{v}{2\pi} = 200$ cps. For these values

$$m = \frac{3.6 \times 10^6}{200}$$

$$= 18{,}000$$

bespeaking approximately 18,000 significant Fourier components[20][23]. It is of more value, and a greater aid to the understanding, to seek a general solution directly by operational methods. The problem has been treated by Laplacian transforms[9], Fourier transforms[12], and unit impulse[11] methods. We shall follow more or less the treatment by Hok[9] using Laplacian transforms, and shall review only the simplest case - the response of a series resonant circuit.

The differential equation for the current in the circuit, excited by a function F(t) is

$$\frac{d^2i}{dt^2} + \frac{R}{L} \cdot \frac{di}{dt} + \frac{1}{LC}\, i = F(t) \quad \text{.....} \quad \text{.....(A.02)}$$

which we may write as

$$Y'' + 2\delta Y' + \omega_o^2 Y = F(t) \quad \text{.....(A.03)}$$

where $\omega_o^2 = \frac{1}{LC}$, $\delta = \frac{R}{2L}$; Y is used for the current function, so that the lower case letter y may be used for the Laplacian transform of Y, $L\{Y\}$

To obtain the corresponding transform equation, write[25]:

$$\begin{aligned} L\{Y''(t)\} &= s^2 y(s) - sY(o) - Y'(o) \\ L\{Y'(t)\} &= sy(s) - Y(o) \end{aligned} \quad \text{.....(A.04)}$$

Let us assume the system initially at rest, so that at $t = 0$, $Y(o) = Y'(o) = 0$

Then substituting in (A.03) the transforms of the derivatives, the transformed equation is

$$s^2 y(s) + 2\delta s\, y(s) + \omega_o^2\, y(s) = f(s)$$

where $f(s) = L\{F(t)\}$

$$\text{Then } y(s) = \frac{f(s)}{s^2 + 2\delta s + \omega_o^2} \quad \text{.....(A.05)}$$

The solution is the inverse transform of this, i.e.,

$$Y(t) = L^{-1}\left\{\frac{f(s)}{s^2 + 2\delta s + \omega_o^2}\right\} \quad \text{.....(A.06)}$$

The inverse transform may be expressed as the convolution integral of the separate inverse transforms, i.e.,

$$Y(t) = \int_o^t F_1(t - \lambda) F(\lambda)\, d\lambda \quad \text{.....(A.07)}$$

where $$F_1(t) = L^{-1}\left\{ \frac{1}{s^2 + 2\delta s + \omega_0^2} \right\} \qquad \text{.....(A.08}$$

This is a well-known form, giving

$$F_1(t) = \frac{e^{-\delta t}}{\omega_1} \left\{ e^{\frac{j\omega_1 t - e^{-j\omega_1 t}}{2j}} \right\} \qquad \text{.....(A.09)}$$

where $\omega_1^2 = \omega_0^2 - \delta^2$

Writing out the convolution integral, we have

$$Y(t) = \frac{1}{2j\omega_1}\left\{ \int_0^t e^{-\delta(t-\lambda)} \left(e^{j\omega_1(t-\lambda)} - e^{-j\omega_1(t-\lambda)} \right) F(\lambda)\, d\lambda \right\}$$

$$= \frac{1}{2j\omega_1}\left\{ e^{-(\delta - j\omega_1)t} \int_0^t e^{(\delta - j\omega_1)\lambda} F(\lambda)\, d\lambda - e^{-(\delta + j\omega_1)t} \int_0^t e^{(\delta + j\omega_1)\lambda} F(\lambda)\, d\lambda \right\}$$

$$= \frac{1}{p_1 - p_2}\left\{ e^{p_1 t} \int_0^t e^{-p_1\lambda} F(\lambda)\, d\lambda - e^{p_2 t} \int_0^t e^{-p_2\lambda} F(\lambda)\, d\lambda \right\}$$

(A.10)

where $p_1 = -(\delta - j\omega_1)$

$p_2 = -(\delta + j\omega_1)$ .....(A.11)

Now, if the decay (relaxation time of the circuit response is less than about $\frac{1}{10}$ the period of the modulation cycle, the frequency of the excitation may be assumed to changing linearly with time[15]. A simple calculation will show that this is a valid assumption for the response of any practical passive network to the cyclotron r-f excitation. Hence we write the decreasing-frequency excitation function as the rotating vector

$$F(t) = E_0\, e^{j(\omega_0 t - \varepsilon t^2)} \qquad \text{.....(A.12)}$$

Differentiation of the vector phase gives the instantaneous angular frequency

$$\hat{\omega} = \omega_0 - 2\varepsilon t \qquad \text{.....(A.13)}$$

We see that $\varepsilon = -\frac{1}{2} \cdot \frac{d\hat{\omega}}{dt}$

Substitution of the explicit F(t) in (A.10) yields the circuit response to the linearly-sweeping-frequency excitation,

$$Y(t) = \frac{E_0}{p_1 - p_2}\left\{ e^{p_1 t}\int_0^t e^{(-p_1 + j\omega_0)\lambda - j\varepsilon\lambda^2} d\lambda \; - e^{p_2 t}\int_0^t e^{(-p_2 + j\omega_0)\lambda - j\varepsilon\lambda^2} d\lambda \right\} \qquad \text{(A.14)}$$

Make the change of variable:

$$\gamma_\nu = \frac{1}{2\varepsilon^{1/2}}(j\omega_0 - p_\nu) - j\varepsilon^{1/2}\lambda \qquad \text{.....(A.15)}$$

where $\nu = 1,2$

The (A.14) becomes

$$Y(t) = \frac{-E_0}{j\varepsilon^{1/2}(p_1 - p_2)}\left\{ e^{p_1 t - \frac{j}{4\varepsilon}(j\omega_0 - p_1)^2}\int_{(\gamma_1)_{t=0}}^{\gamma_1} e^{j\gamma_1^2} d\gamma_1 \right.$$

$$\left. - e^{p_2 t - \frac{j}{4\varepsilon}(j\omega_0 - p_2)^2}\int_{(\gamma_2)_{t=0}}^{\gamma_2} e^{j\gamma_2^2} d\gamma_2 \right\} \qquad \text{((A.16)}$$

Outside the integral, put (from (A.15)),

$$-\frac{j}{4\varepsilon}(j\omega_0 - p_\nu)^2 = (j\omega_0 - p_\nu)t - j\varepsilon t^2 - j\gamma_\nu^2 \qquad \text{(A.17)}$$

Then we obtain

$$Y(t) = \frac{-E_0 e^{j(\omega_0 t - \varepsilon t^2)}}{j\varepsilon^{1/2}(p_1 - p_2)}\left\{ e^{-j\gamma_1^2}\int_{(\gamma_1)_0}^{\gamma_1} e^{j\gamma_1^2} d\gamma_1 - e^{-j\gamma_2^2}\int_{(\gamma_2)_0}^{\gamma_2} e^{j\gamma_2^2} d\gamma_2 \right\} \qquad \text{(A.18)}$$

or, putting $p_1 - p_2 = 2j\omega_1$ (A.11)

$$Y(t) = \frac{E_0 e^{j(\omega_0 t - \varepsilon t^2)}}{2\omega_1 \varepsilon^{1/2}} \left\{ e^{-j\gamma_1^2} \int_{(\gamma_1)_0}^{\gamma_1} e^{j\gamma_1^2} d\gamma_1 - e^{-j\gamma_2^2} \int_{(\gamma_2)_0}^{\gamma_2} e^{j\gamma_2^2} d\gamma_2 \right\} \tag{A.19}$$

This represents the original excitation vector modified by a factor made up of complex Fresnel integrals. As t goes from o to ∞ along the real axis the variable γ moves along a straight line in the complex plane parallel to the j-axis, i.e, along the line $x = \frac{\delta}{2\varepsilon^{\frac{1}{2}}}$ from the values

$$\left.\begin{aligned} (\gamma_1)_{t=0} &= \frac{\delta}{2\varepsilon^{1/2}} + j\left(\frac{\omega_0 - \omega_1}{2\varepsilon^{1/2}}\right) \\ \text{and} \quad (\gamma_2)_{t=0} &= \frac{\delta}{2\varepsilon^{1/2}} + j\left(\frac{\omega_0 + \omega_1}{2\varepsilon^{1/2}}\right) \end{aligned}\right\} \tag{A.20}$$

to $\gamma = \frac{\delta}{2\varepsilon^{1/2}} - j\infty$

Some of these integrals have been computed by Hok[9] for the increasing-frequency case, giving response shapes similar to the one sketched in fig. 14. He lists suitable expansions for their evaluation. The decreasing-frequency response differs slightly from the increasing-frequency response, as shown by Lewis[14], and as evident in the photographs figs. 13(a) and (b). The difference is greatest for the slower sweep rates since it arises from a difference in direction of integration along the above contour from the same initial points (A.20). Methods of evaluating integrals equivalent to the above have been given by Lewis[14], Barber and Ursell[10], and Clavier[12]. Hok, and Barber and Ursell, have plotted the response curves in dimensionless coordinates, showing that the character of the response is determined by the real part of

i.e. $\frac{\delta}{2\varepsilon^{\frac{1}{2}}} = \alpha$. The imaginary part determines the time scale. The dimensionless "time" variable is $\beta = \varepsilon^{\frac{1}{2}} t$.

APPENDIX B

THE NON-LINEAR DIFFERENTIATING CIRCUIT

For the circuit of constant C and constant R (fig. 15a) it is easily shown that, if V_1 is a linearly rising voltage

$$V_1 = \alpha t$$

applied across the network, then the voltage V appearing across R is

$$V = RC\alpha(1 - e^{-\frac{1}{RC}t}) \qquad \text{.....(1)}$$

The maximum value of V, as t becomes very large, is

$$V_{max} = RC\alpha \qquad \text{.....(2)}$$

That is, V_{max} is directly proportional to the rate of rise of the voltage V_1 for a differentiating circuit of constant R.

Consider now the circuit of fig. 15(b), where R has been replaced by a diode through which is flowing a small bias current i_o, through a high resistance R_o to a positive potential. For small values of i_o, the anode potential will be negative with respect to the cathode, owing to the initial velocity of electrons emitted from the cathode. In this region of negative anode potentials the current-voltage relation for the diode is well approximated by[8][26]

$$i = ae^{bV} \qquad \text{.....(3)}$$

We shall assume this law for the diode in place of Ohm's law for the constant resistor. In addition we shall make the simplifying assumption that i_o is constant. This will be valid if the voltage changes across the diode are small compared to the voltage drop across R_o; this condition is met in the application.

Then we may write

$$i = i_o + i_1 \qquad \text{.....(4)}$$

$$V_1 = \int \frac{i_1}{C}\,dt + V \qquad \ldots\ldots\ldots\ldots\ldots\ldots\ldots\ldots\ldots\ldots(5)$$

$$V_1 = \alpha t \qquad \ldots\ldots\ldots\ldots\ldots\ldots\ldots\ldots\ldots\ldots\ldots\ldots(6)$$

where i is the current through the diode, V the voltage across it; i_1 and V_1 are the current and voltage from the source, and V_1 is assumed a linearly rising voltage as before.

Substituting (6) in (5), and differentiating with respect to t,

$$\frac{dV}{dt} = \alpha - \frac{i_1}{C}$$

$$= \alpha + \frac{i_o}{C} - \frac{i}{C}$$

$$\text{or} \quad \frac{dV}{C\alpha + i_o - i} \qquad \ldots\ldots\ldots\ldots\ldots\ldots\ldots\ldots\ldots\ldots\ldots\ldots(7)$$

Substitute (3) and integrate both sides:

$$\int \frac{dV}{C\alpha + i_o - ae^{bV}} = \int \frac{dt}{C} \qquad \ldots\ldots\ldots\ldots\ldots\ldots\ldots(8)$$

The integral on the left is a standard form, giving

$$\frac{1}{C\alpha + i_o}\left[V - \frac{1}{b}\cdot \log\left(C\alpha + i_o - ae^{bV}\right)\right] = \frac{t}{C} + K \qquad \ldots\ldots\ldots(9)$$

From the initial conditions $t = 0$, $i = i_o$

$$K = \frac{1}{b(C\alpha + i_o)}\left[\log \frac{i_o}{C\alpha}\right] \qquad \ldots\ldots\ldots\ldots\ldots(10)$$

Rearrangement of (9) then gives

$$V = \frac{1}{b}\log\left[\frac{i_o}{a}\,\frac{\left\{\frac{i_o}{c} + \alpha\right\}}{\left\{\frac{i_o}{C} + \alpha e^{-b\left(\frac{i_o}{C} + \alpha\right)t}\right.}\right] \qquad \ldots\ldots\ldots\ldots\ldots(11)$$

For convenience, introduce the quantities

$$\beta = \frac{C \alpha}{i_o} \qquad \text{.....(12)}$$

$$T = \frac{i_o}{C} t$$

Then

$$V = \frac{1}{b} \log \left[\frac{i_o}{a} \frac{(\beta + 1)}{\{1 + \beta e^{-(\beta + 1)bT}\}} \right] \qquad \text{.....(13)}$$

When T becomes very large,

$$V_{max} = \frac{1}{b} \log \left[\frac{i_o}{a} (\beta + 1) \right] \qquad \text{for } \beta > -1 \qquad \text{.....(14)}$$

To assess the discrimination between voltages rising at different rates, find

$$\frac{dV_{max}}{d\beta} = \frac{1}{b(\beta + 1)} \qquad \text{.....(15)}$$

This is a hyperbola, approaching infinity as β approaches -1. (Compare the straight line $\frac{dV_{max}}{d\alpha} = RC$ for the linear case). For $\beta > -1$, V is asymptotic to the value given by (14). For $\beta = -1$, V ceases to be asymptotic to a constant value, and continues to fall indefinitely with V_1, as given by the equation.

$$\lim_{\beta \to -1} V = \frac{-1}{b} \log \frac{a}{i_o} (1 + bT) \qquad \text{.....(16)}$$

For $\beta < -1$ it is easily shown from (13) that V approaches V_1 as $|\beta|$ becomes large. In other words, for a large amplitude of input pulse, the discrimination between rates of fall is very great for $\alpha \to -\frac{i_o}{C}$. For rates of fall slower than $\frac{i_o}{C}$ the output V is asymptotic to a constant (low) value (equation 14) and for rates of fall faster than $\frac{i_o}{C}$ the output V approaches the input voltage V_1.

In the application to the frequency triggering circuit (fig. 6, Chapter IV) the anode of the diode is replaced by the control grid of the 6AC7. Fig. 16 shows the grid-current vs. grid-voltage curves for a number of 6AC7 tubes picked at random. The heavier line is an estimated representative curve. The current is plotted on a logarithmic scale so that the relation (3) would be a straight line. It may be seen that this relation is a fair approximation for currents below 50 μamperes, i.e., in the grid voltage region -0.9 to -0.5 volts. Evaluating the constants from this region of the graph, we get

$$a = 1410 \ \mu\text{amperes}$$

$$b = 7.6 \ \text{volts}^{-1}$$

As an example, to discriminate with maximum efficiency between the pulse from the filter edge in (IV,4) and a less steeply falling pulse, adjust $-\frac{i_o}{C}$ to be approximately equal to α for this case.

Frequency width of edge = 0.12 Mc/s

Amplitude of pulse from detector as measured = 10 v

$$\frac{df}{dt} \text{ at } 25.0 \text{ Mc/s} = \frac{3.32 \times 10^{10}}{2\pi} \ \text{c/s}^2$$

$$\therefore \quad = 10 \times \frac{3.32 \times 10^{10}}{2\pi \times 0.12 \times 10^{6}}$$

$$= 4.4 \times 10^{5} \ \text{volts/sec.}$$

If we set i_o at a mean value of 50 μamperes (this is made adjustable for best operating conditions in practice), we obtain, for C

$$C = \frac{i_o}{\alpha}$$

$$= \frac{50 \times 10^{-6}}{4.4 \times 10^{5}}$$

$$= 110 \ \mu\mu f$$

The discrimination between the pulses from the filter is increased still further by a fortunate added effect from the rising edge of the pulse which shortly precedes the all-important falling edge. In the case of the unwanted pulse the rising edge is the steeper and therefore causes a larger positive voltage on the grid than is the case for the wanted pulse, of which the slower edge comes first. As a result, the assumption that $i = i_o$ at $t = 0$ (the start of the falling portion) is not quite true - the negative drop of the unwanted pulse starts at effectively a higher value of i_o and suffers an added attenuation. While it is not necessary for the required degree of discrimination, this added effect is useful in making the adjustment of i_o/C less critical so that the circuit operates satisfactorily over a wide range of modulating frequencies and, in the case of the oscilloscope triggering circuit, over the range of different slopes on the side of the modulating waveform.

APPENDIX C

THE ION SOURCE PULSE GATING SYSTEM

The following notes are appended as a guide to the circuit diagram, fig. 7.

T_1 - the trigger generating thyratron. Its cathode is connected to the cable to the cyclotron room by the relay R, energized by the "Pulse Ion Source" button on the control panel. The cable is terminated by a 120 ohm resistor at the cyclotron room end. The pulses from the selective frequency trigger circuit (fig. 6) arrive continuously at the control grid, and at the control grids of

T_2 and T_3. T_2 is an isolating cathode follower feeding the pulses to the modulation frequency meter circuit (fig. 12). T_3 is a cathode follower matching the Delay Line which delays the pulses about 1 μ sec before they reach the control grid of

T_4, the resetting thyratron. The switches in plate and grid circuits determine its operation in the different modes described in (IV,5). The negative pulse from the anode of T_4 is coupled to the anode of T_1 by a 0.005 μf condenser, smaller than C_1 and C_4 so that the firing of T_1 will not draw too much charge from C_4 and thus reduce the amplitude of the extinguishing pulse. A 120 ohm resistor is placed in series with C_1 so that the extinguishing pulse from the anode of T_4 will not be effectively short circuited to earth. A pulse from the cathode of T_4 is used to trigger

T_5, a square pulse generator supplying a negative pulse to the second control grid of T_1 to assist in extinguishing the ionization

and to prevent its being triggered again by the pulses on the first control grid until the condenser C_1 is fully charged to the clamped value of 100 volts.

T_6 and T_7 are diodes clamping the maximum anode voltages of the two thyratrons at + 100 volts so that (1) the amplitude of pulses generated by the discharge of the condensers will always be the same, and (2) the charging time is reduced since the condensers charge through R_1 and R_4 toward a potential of + 250 volts.

REFERENCES

(1). W.M. Telford, Thesis, McGill University, Aug. 31, 1949.

(2). D. Bohm and L. Foldy, "Theory of the Synchro-cyclotron", Phys. Rev., 72, 649, (1947).

(3) L.R. Henrich, D.C. Sewell, J. Vale, "Operation of the 184-inch Cyclotron", R.S.I., 20, 887, (1949).

(4) Richardson, Wright, Lofgren, and Peters, "Development of the Frequency Modulated Cyclotron", Phys. Rev., 73, 5, (1948).

(5) D.W. Hone, Thesis, McGill University, in preparation.

(6) Terman, Radio Engineer's Handbook, page 353, McGraw-Hill.

(7) V.L. Fitch and E.W. Titterton, "A Laboratory Oscilloscope", R.S.I., 18, 11, (1947).

(8) Arguimbau, Vacuum-Tube Circuits, Wiley.

(9) G. Hok, "Response of Linear Resonant Systems to Excitation of a Frequency Varying Linearly with Time", J.App. Phys., 19, 242, (March 1948).

(10) N.F. Barber and F. Ursell, "The Response of a Resonant System to a Gliding Tone", Phil. Mag., 39, 292, 345, (May, 1948).

(11) N.F. Barber, "The Optimum Performance of a Wave Analyzer", Electronic Eng. (London), 21, 175, (May, 1949).

(12) A.G. Clavier, "Application of Fourier Transforms to Variable-Frequency Circuit Analysis", Proc. I.R.E., 37, 1287, (Nov. 1949).

(13) W.H. Hamilton, "Response of a Tuned Amplifier to a Signal Varying Linearly in Frequency", Proc. National Electronics Conference (Chicago), 4, 377, (1948).

(14) F.M. Lewis, "Vibration during acceleration through a critical speed", Trans. Am. Soc. Mech. Eng., APM 54-24, 253, (1932)

(15) B.A. Jacobsen and R.K. Wangsness, "Shapes of nuclear Induction Signals", Phys. Rev., 73, 942, (May 1, 1948).

(16) J.R. Carson and T.C. Fry, "Variable Frequency Electric Circuit Theory with Application to the Theory of Frequency Modulation", Bell. Syst. Tech. Jour, 16, 513, (Oct. 1937).

(17) H. Roder, "Effect of Tuned Circuits on an F-M Signal", Proc., I.R.E., 25, 1617, (Dec. 1937).

(18) Cherry and Rivlin, "Non-linear Distortion, with Particular Reference to the Theory of Frequency-Modulated Waves", Phil. Mag. 32, 265, (1941); Phil. Mag. 33, 272, (1942).

(19) D.L. Jaffe, "A theoretical and experimental investigation of tuned circuit distortion in Frequency-Modulated Systems"., Proc. I.R.E., 33, 318, (May, 1945).

(20) W.J. Frantz, "Transmission of an F-M Wave through a Network", Proc. I.R.E., 34, 114, (Mar. 1946).

(21) B. van der Pol,"The Fundamental Principles of Frequency Modulation", Jour. I.E.E. (London) part III, 93, 153, (May 1946).

(22) A.S. Gladwin, "The Distortion of Frequency-Modulated Waves by Transmission Networks", Proc. I.R.E., 35, 1436, (Dec. 1947).

(23) B. Gold, "The Solution of Steady-State Problems in F-M". Proc. I.R.E., 37, 1264, (Nov. 1949).

(24) Goldman, "Frequency Analysis, Modulation, and Noise, McGraw-Hill, 1948.

(25) Churchill,"Modern Operational Mathematics in Engineering, McGraw-Hill, 1944.

(26) Reich, "Theory and Applications of Electron Tubes", McGraw-Hill.

(27)

Bibliography on Filter Design.

Terman, Radio Engineer's Handbook

Bode, Network Analysis and Feedback Amplifier Design.

Guillemin, Communication Networks , Vol. II.

Golay, "The Ideal Low-pass Filter in the Form of a Dispersionless Lag Line", Proc. I.R.E., 34, 138, (March 1946).

M. Dishal, "Design of Dissipative Band-pass filters Producing Desired Exact Amplitude-Frequency Characteristics". Proc. I.R.E., 37, 1050, (Sept. 1949).

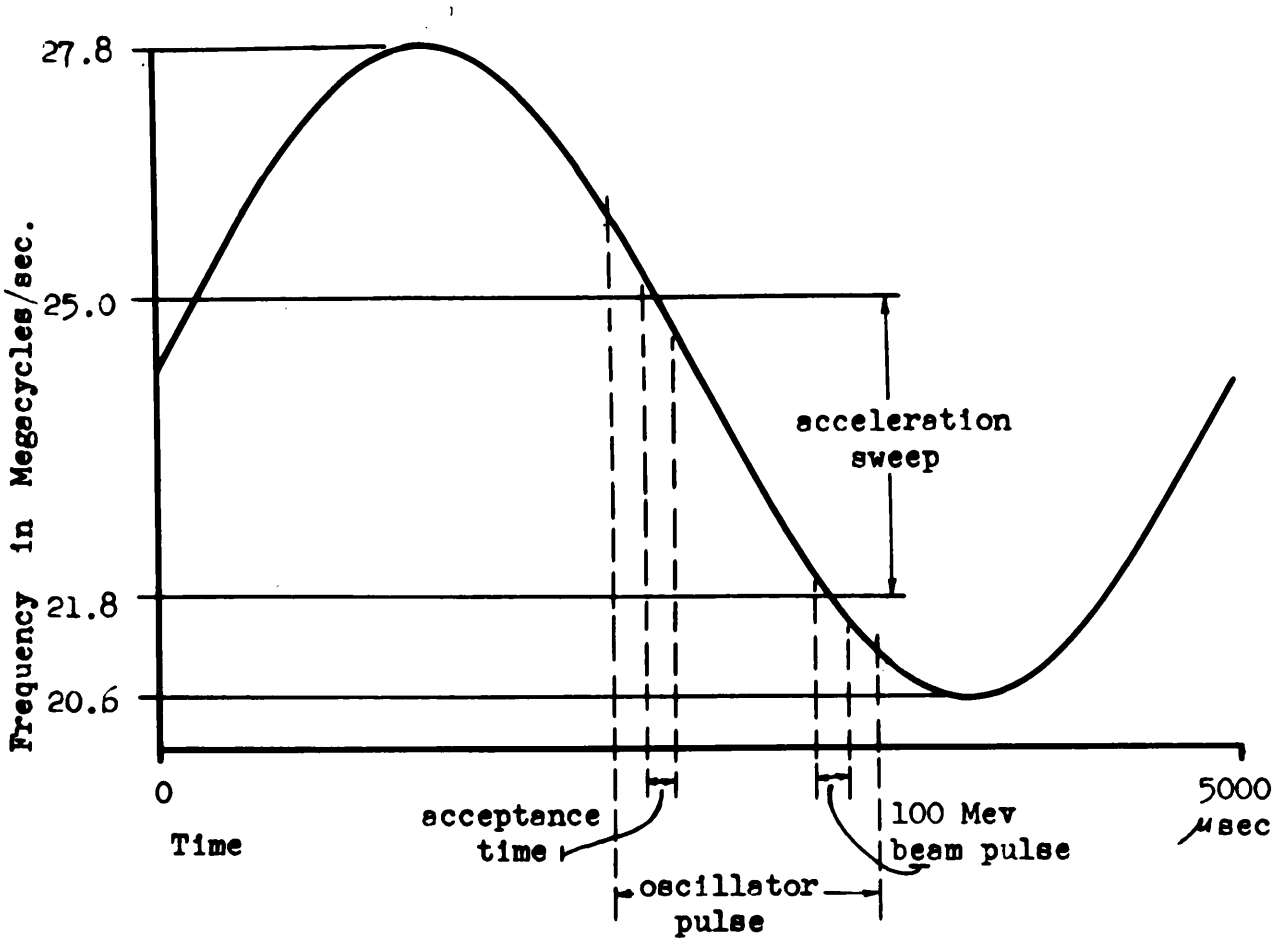

Fig.1. McGill cyclotron frequency modulation cycle.

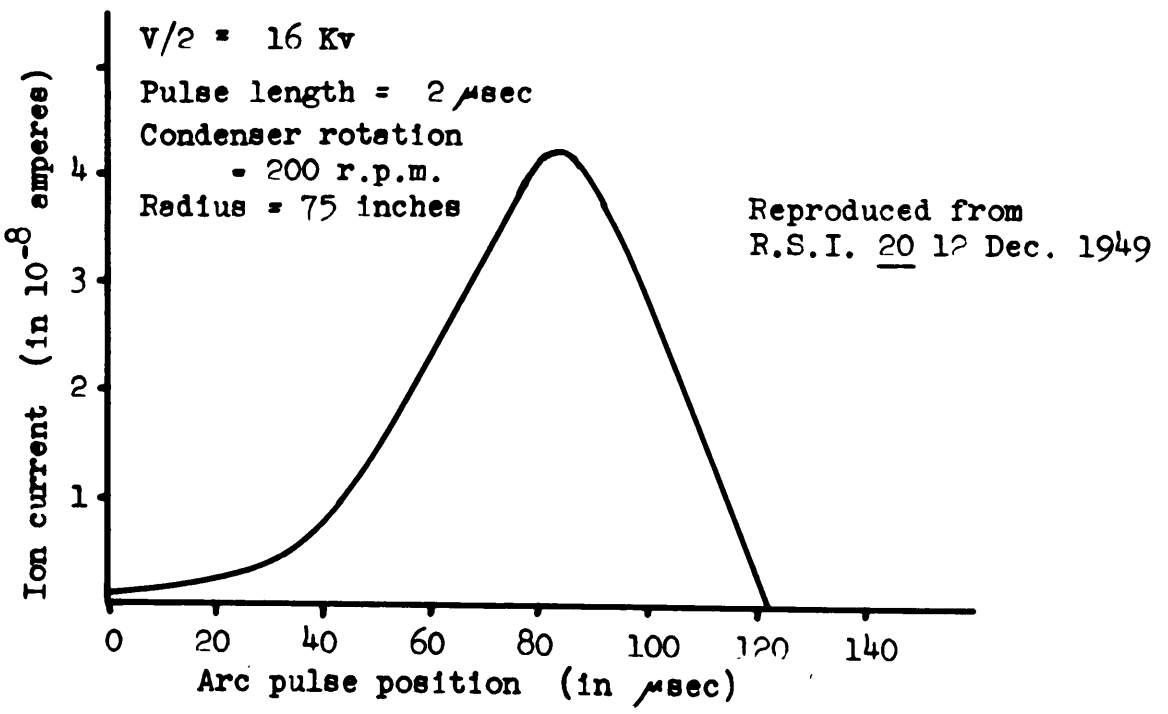

Fig.2. Berkeley measurement of ion current at target as a function of ion source pulse position.

a) Responses of a resonant circuit of Q about 1200 to the increasing (left) and decreasing (right) frequency sweeps of the f-m cyclotron signal.

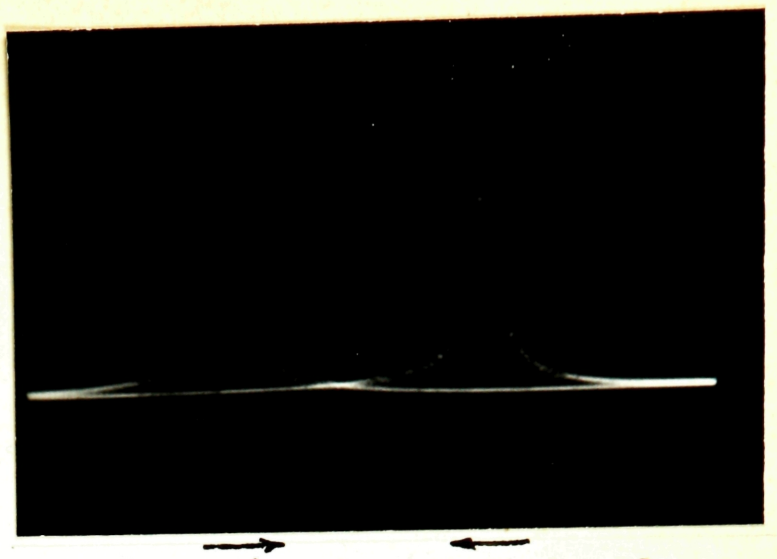

b) Same as a) at a modulating frequency of 100 cps. The direction of increasing time is shown by the arrows.

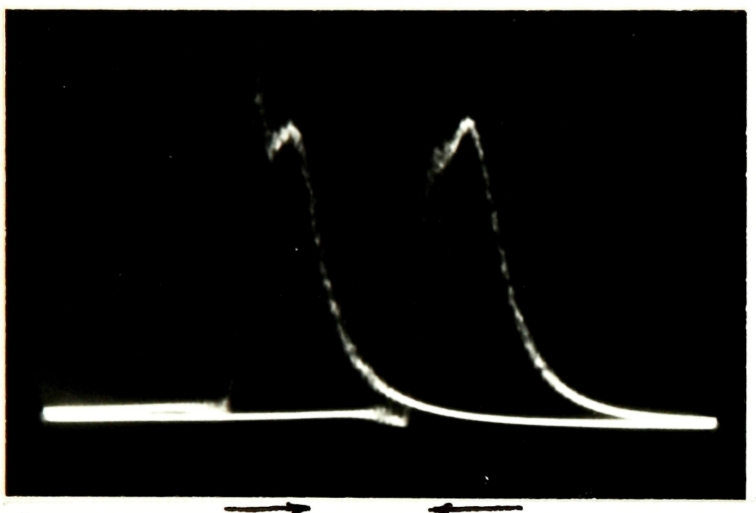

c) The band-pass filter characteristic. The frequency scale is from left to right.

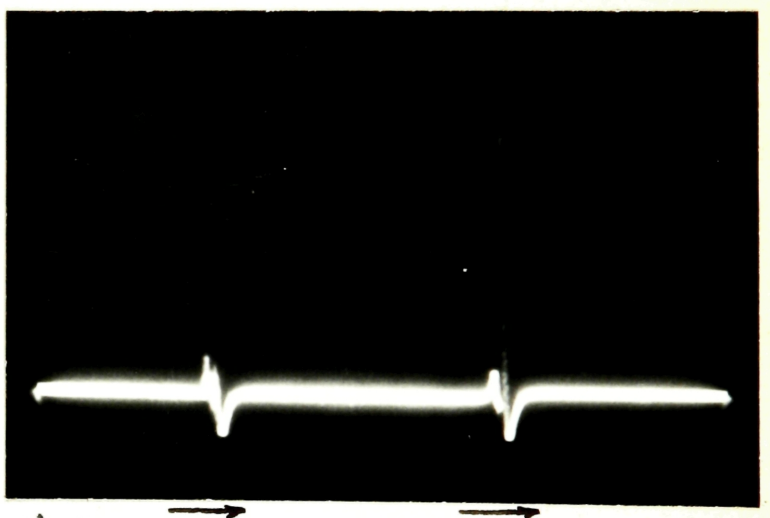

d) The pulses derived from the filter response envelopes after discrimination - on a time base.

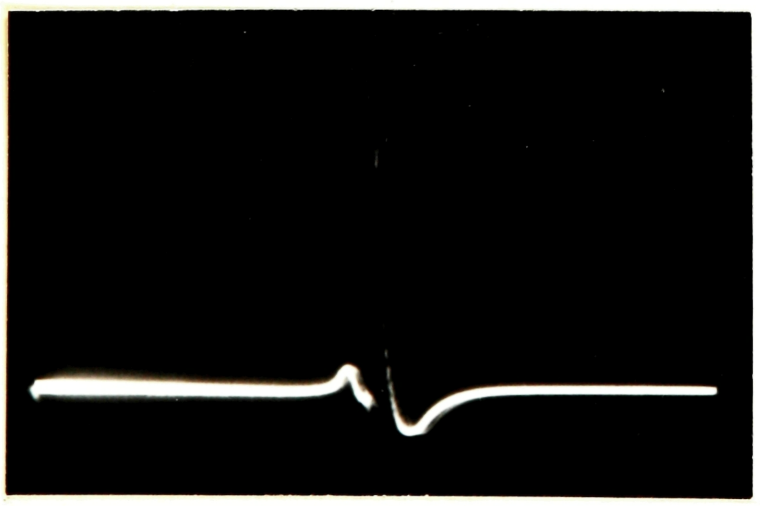

e) A closer look at the right hand pulse of d)

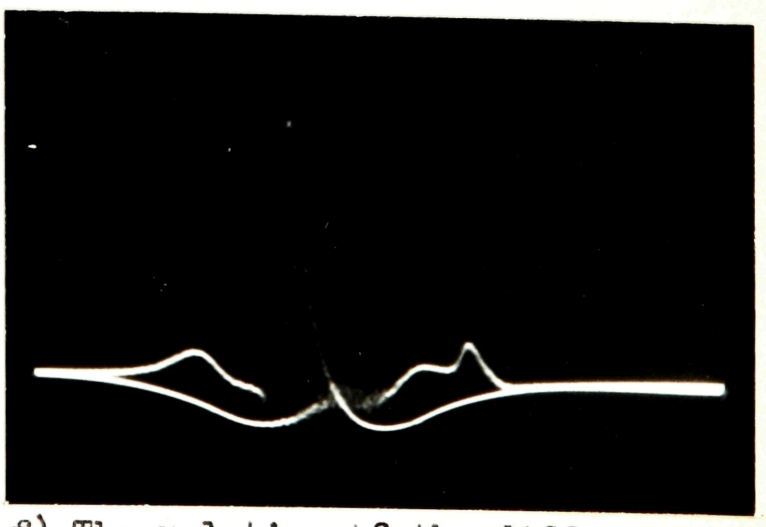

f) The relation of the differentiated pulses to the filter responses of c). The scales have been reversed.

Figure 3

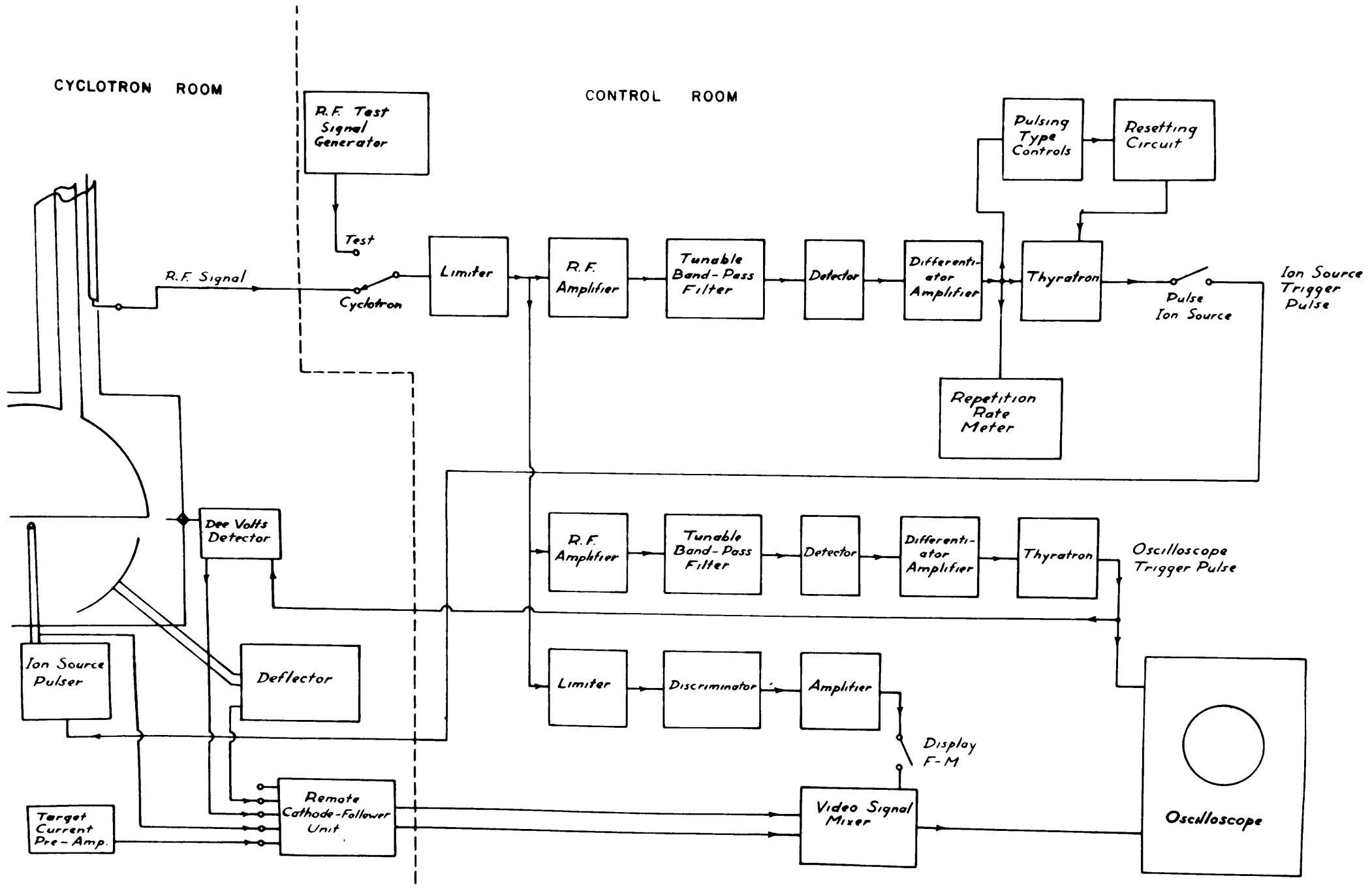

FIG. 4. SCHEMATIC DIAGRAM OF CYCLOTRON SYNCHRONIZING AND MONITORING CIRCUITS.

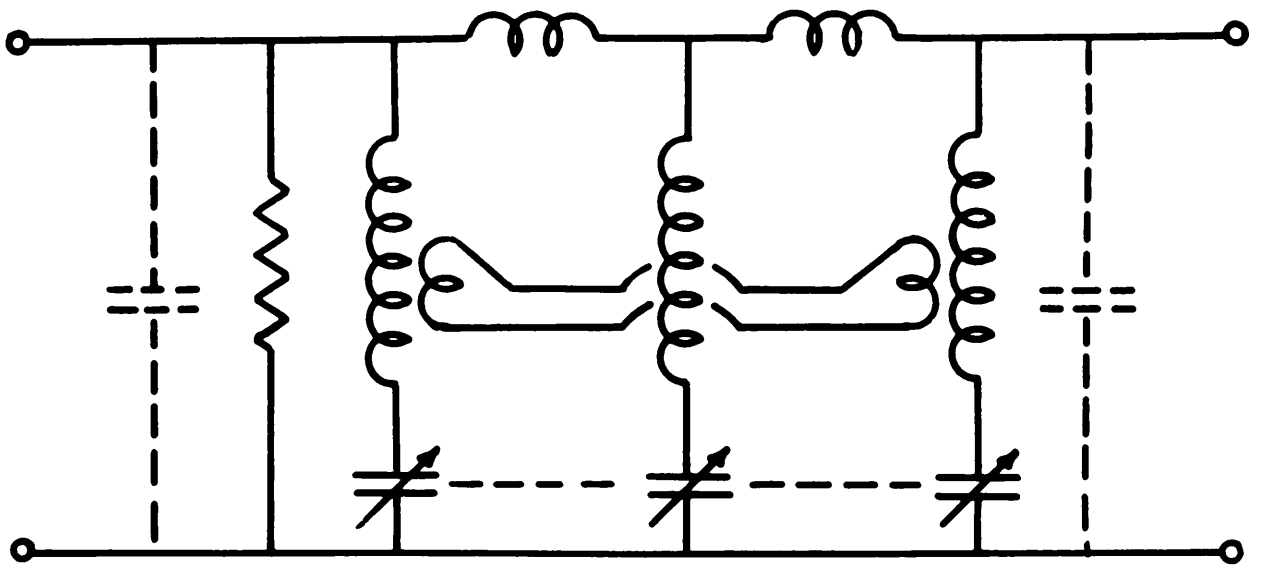

Fig.5(a).

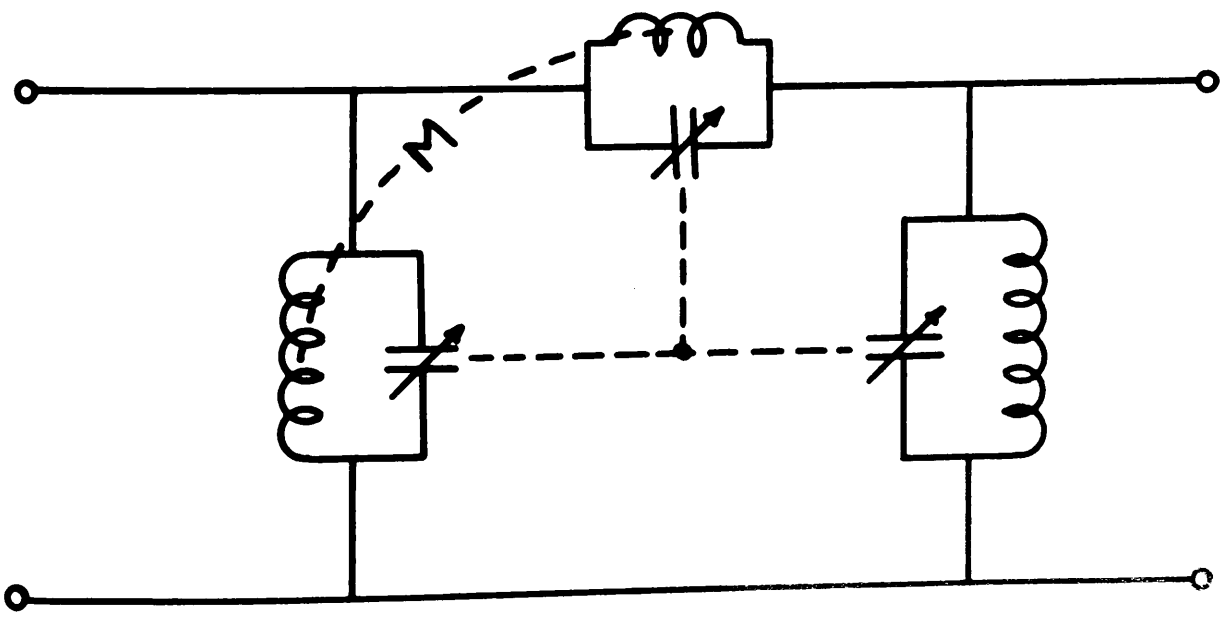

Fig.5(b).

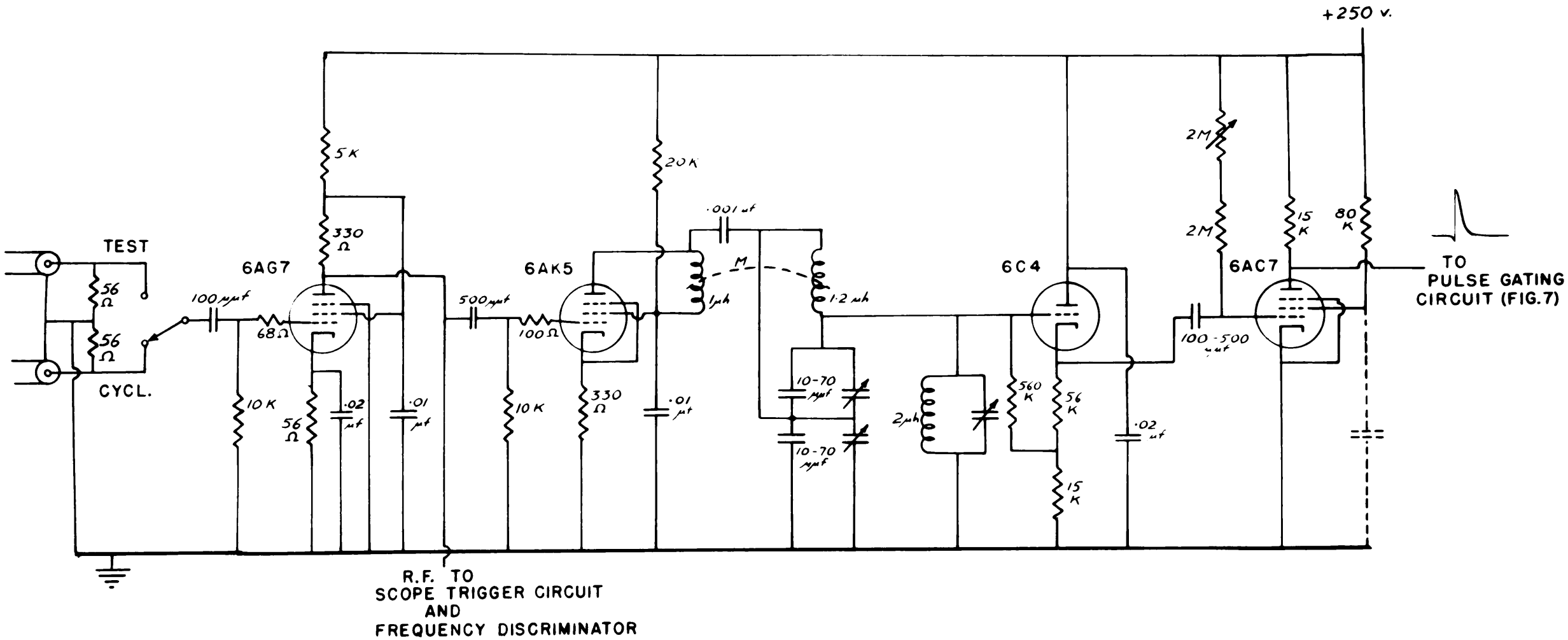

FIG. 6. R.F. TRIGGER CIRCUIT FOR ION SOURCE PULSE

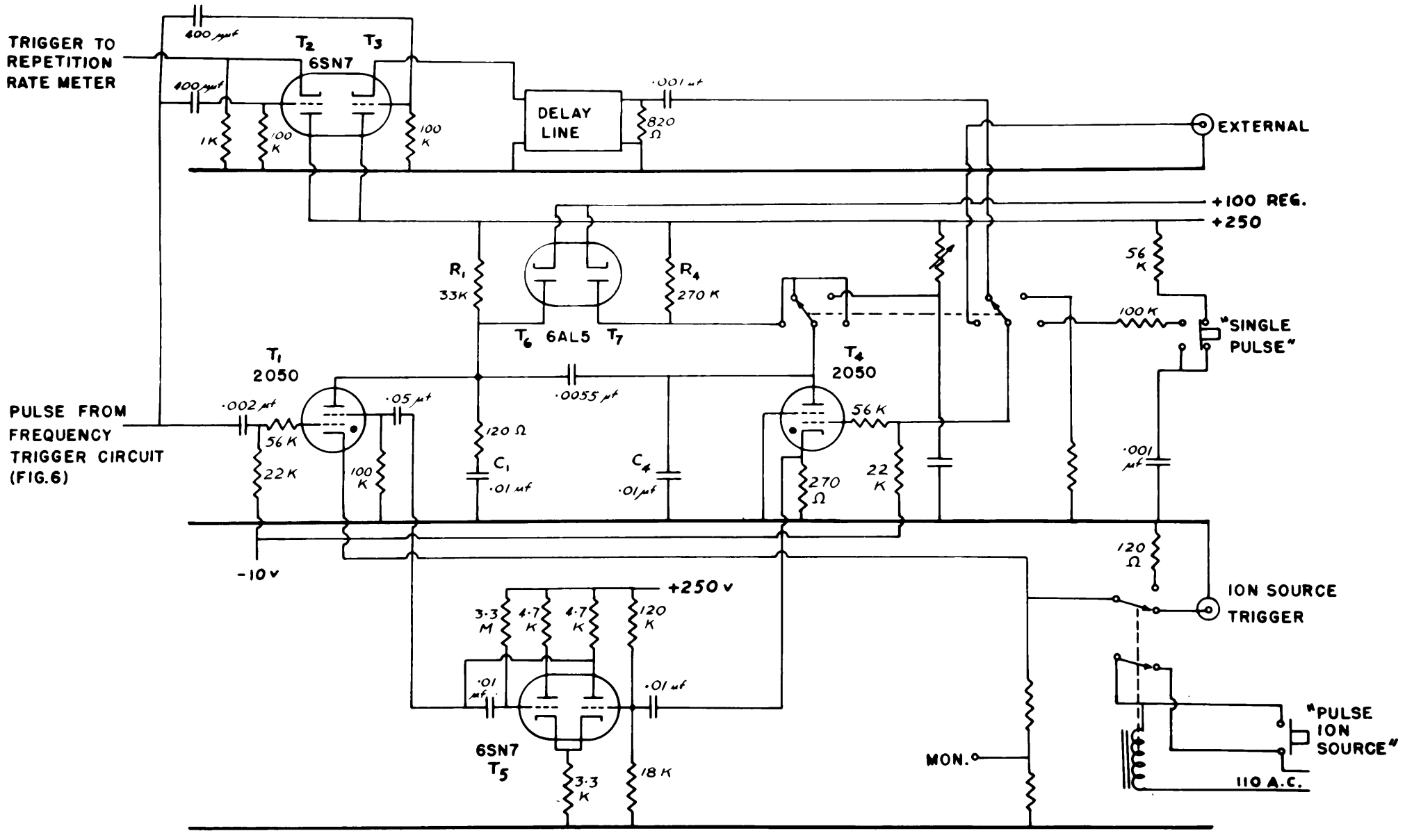

FIG. 7. PULSE GATING CIRCUIT.

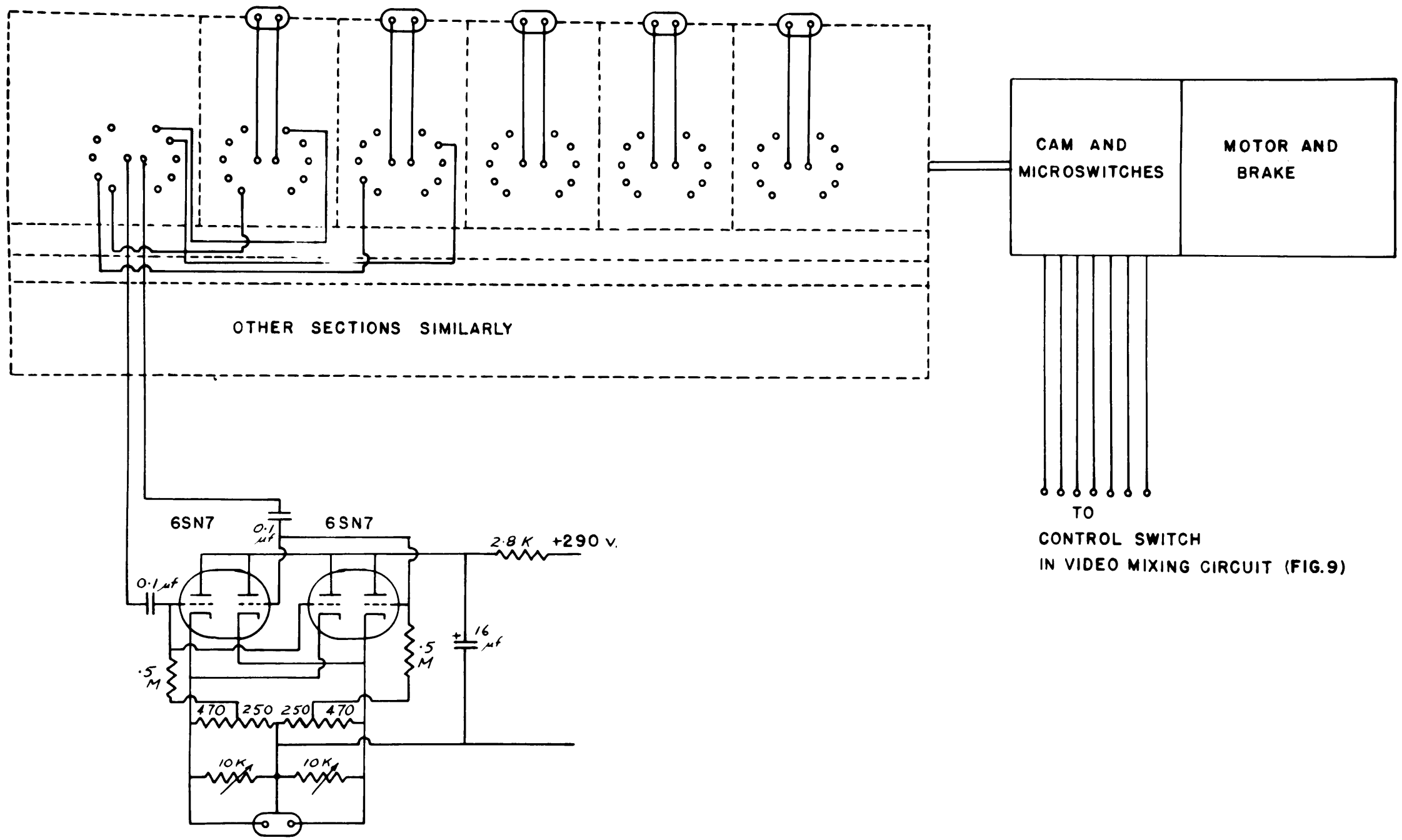

FIG. 8. REMOTE SWITCH AND CATHODE FOLLOWER UNIT.

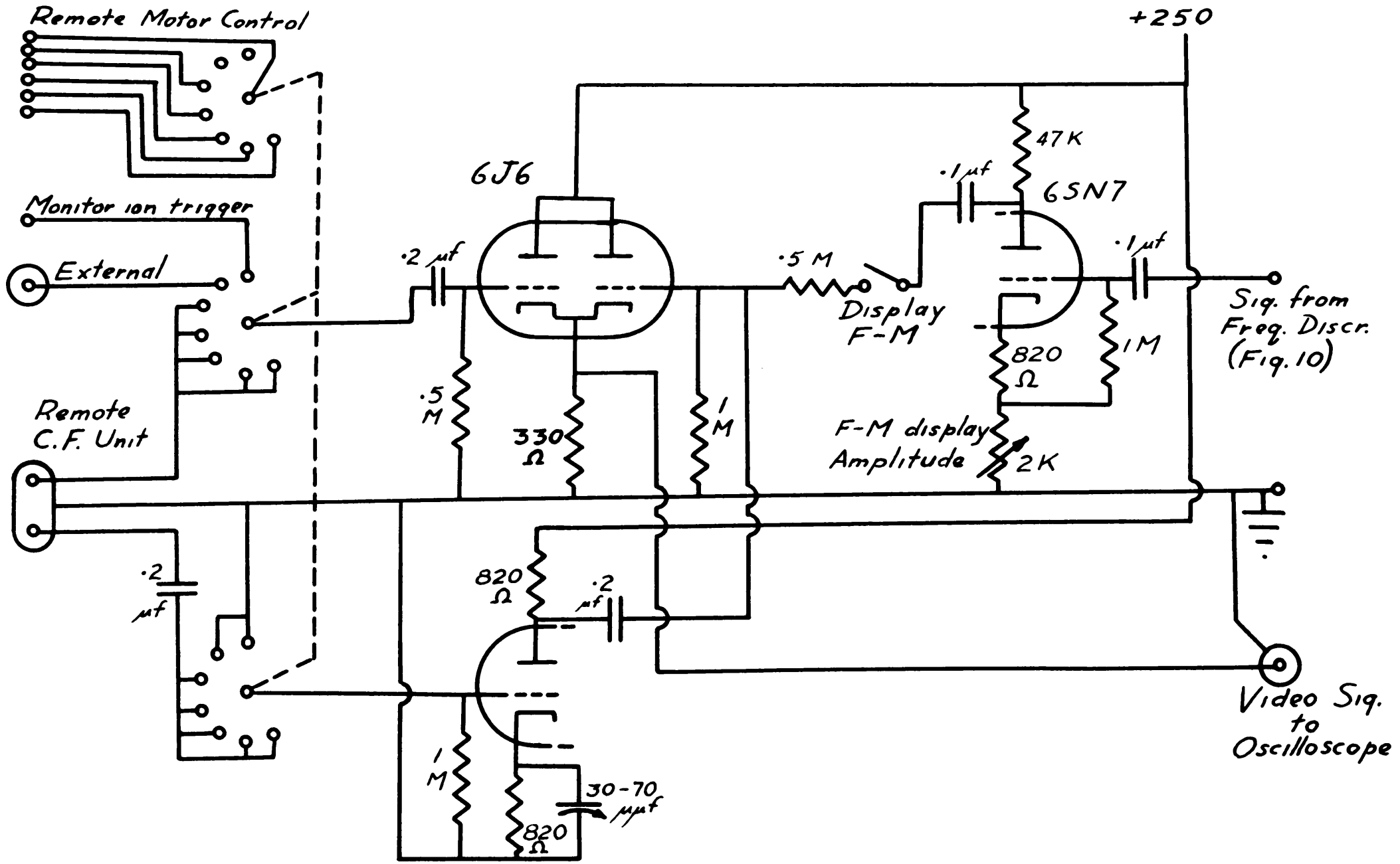

Fig.9. Video Signal Mixer.

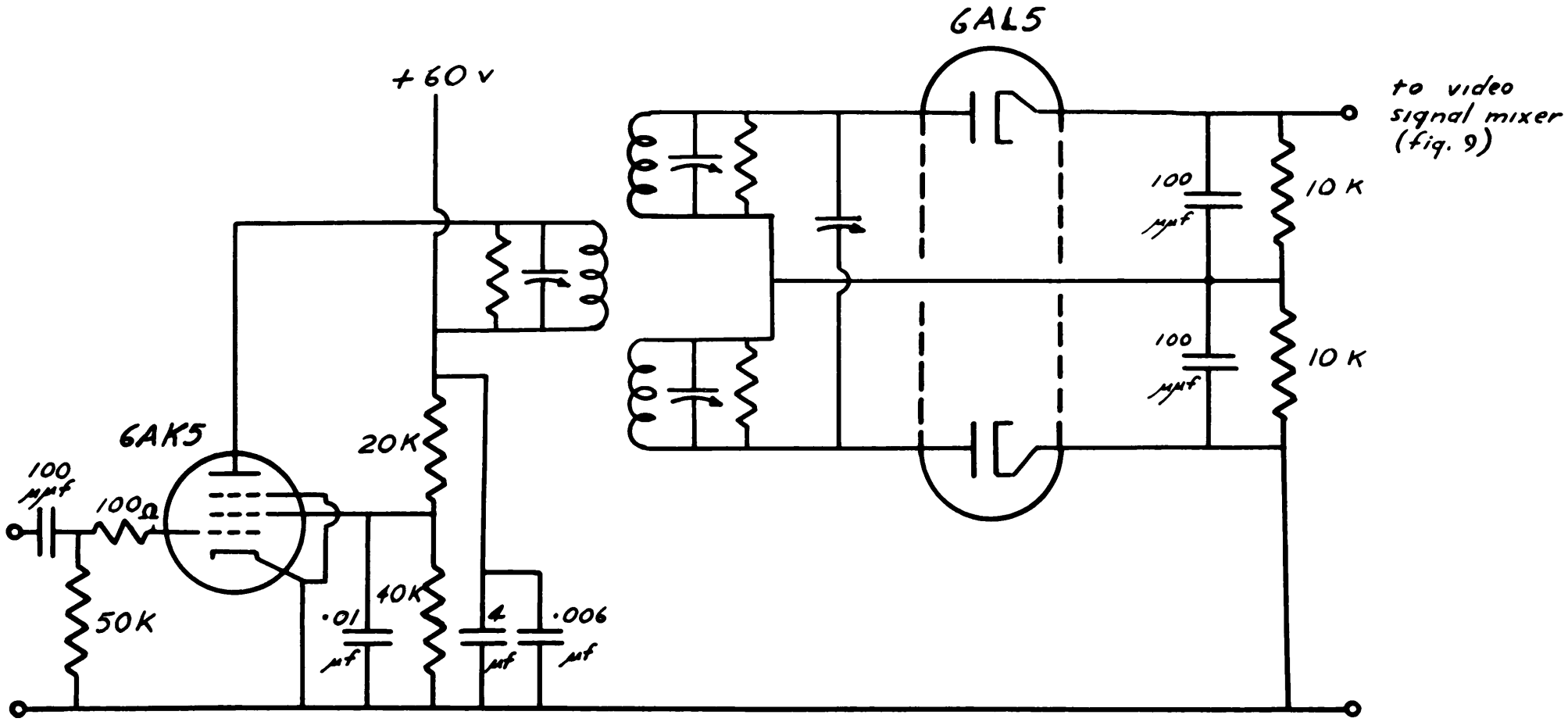

Fig.10. Limiter and Frequency Discriminator.

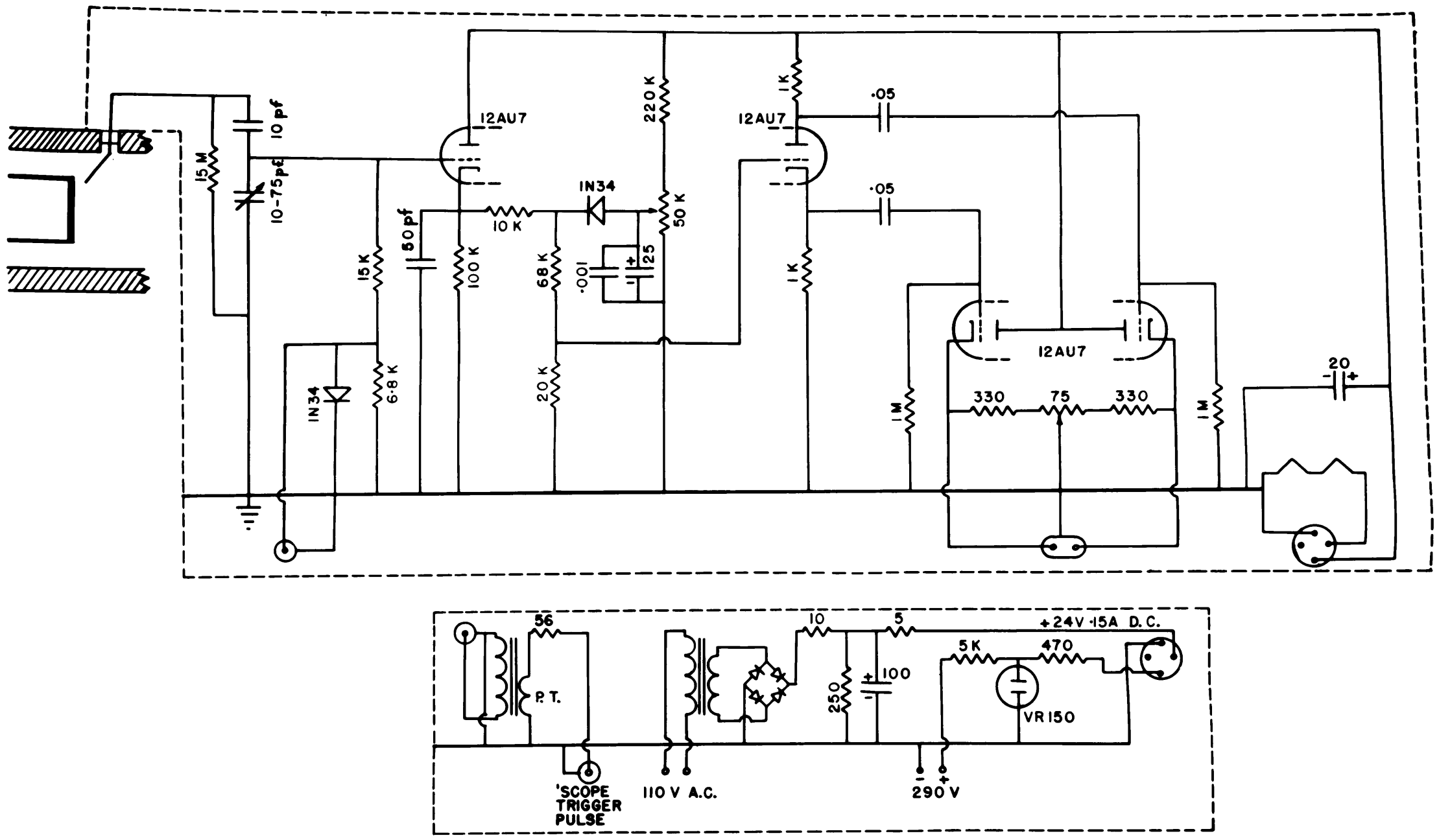

FIG.11. R.F. DEE VOLTAGE DETECTOR CIRCUIT.

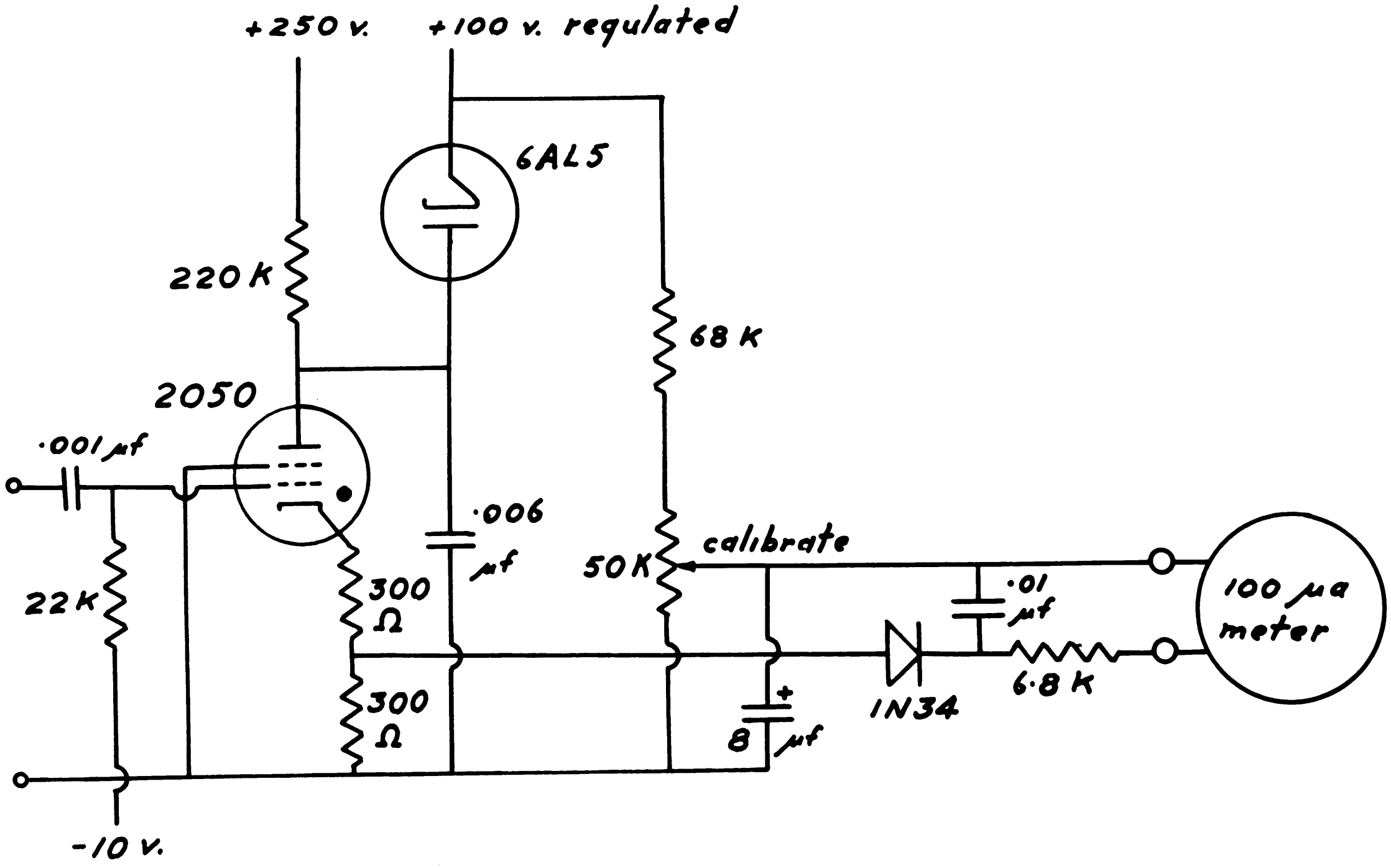

Fig.12. Repetition Rate Meter.

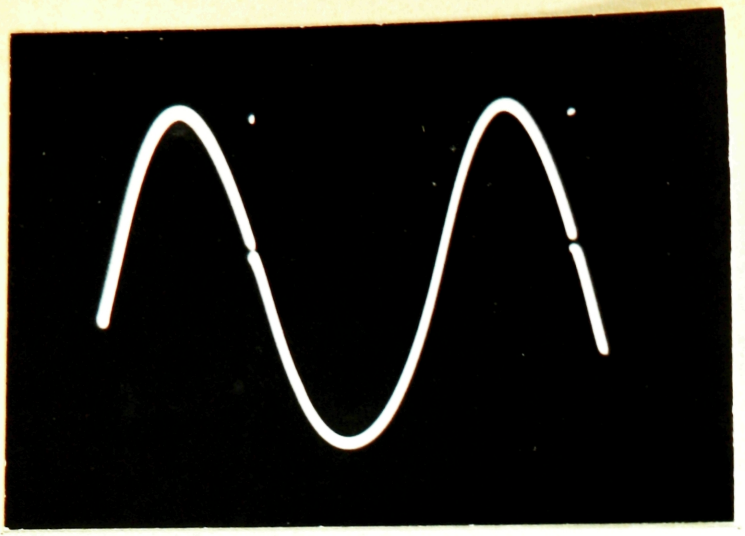

a) Ion source current pulse displayed on frequency vs time curve.

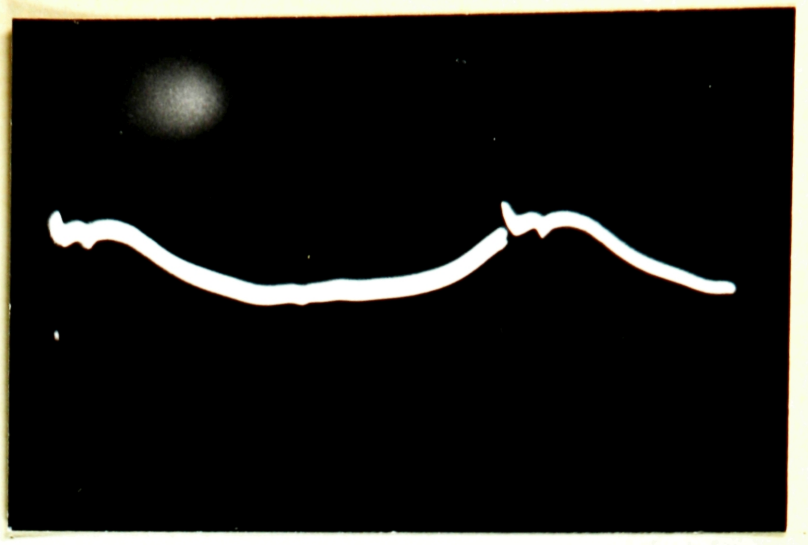

b) Dee voltage vs time.

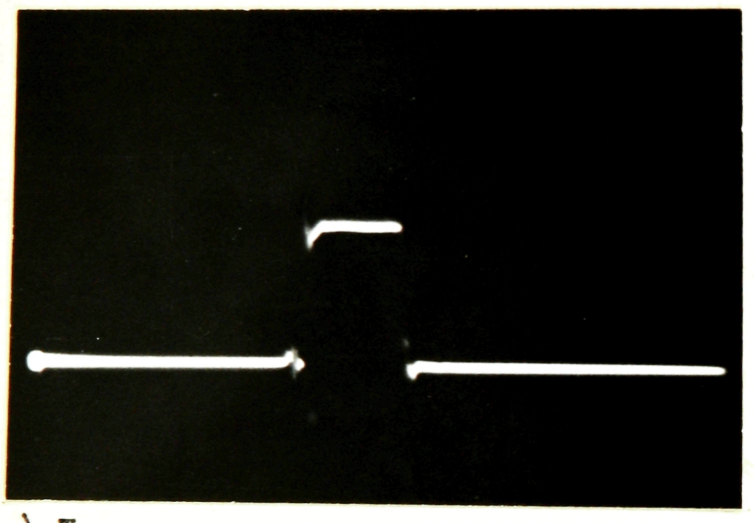

c) Ion source current pulse.
Length ≈ 50 μsec.

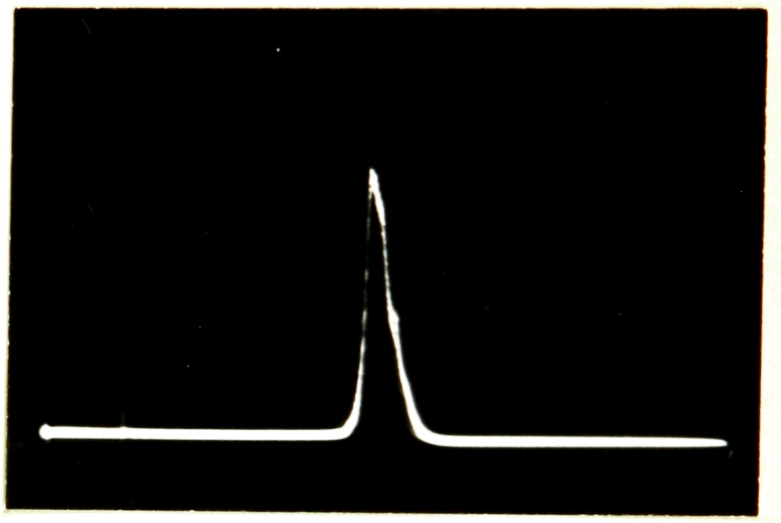

d) Integrated target current pulse. V/2 = 8 kv
repetition rate = 200 cps
Dee bias 1100 v.

Figure 13

Oscilloscope Displays

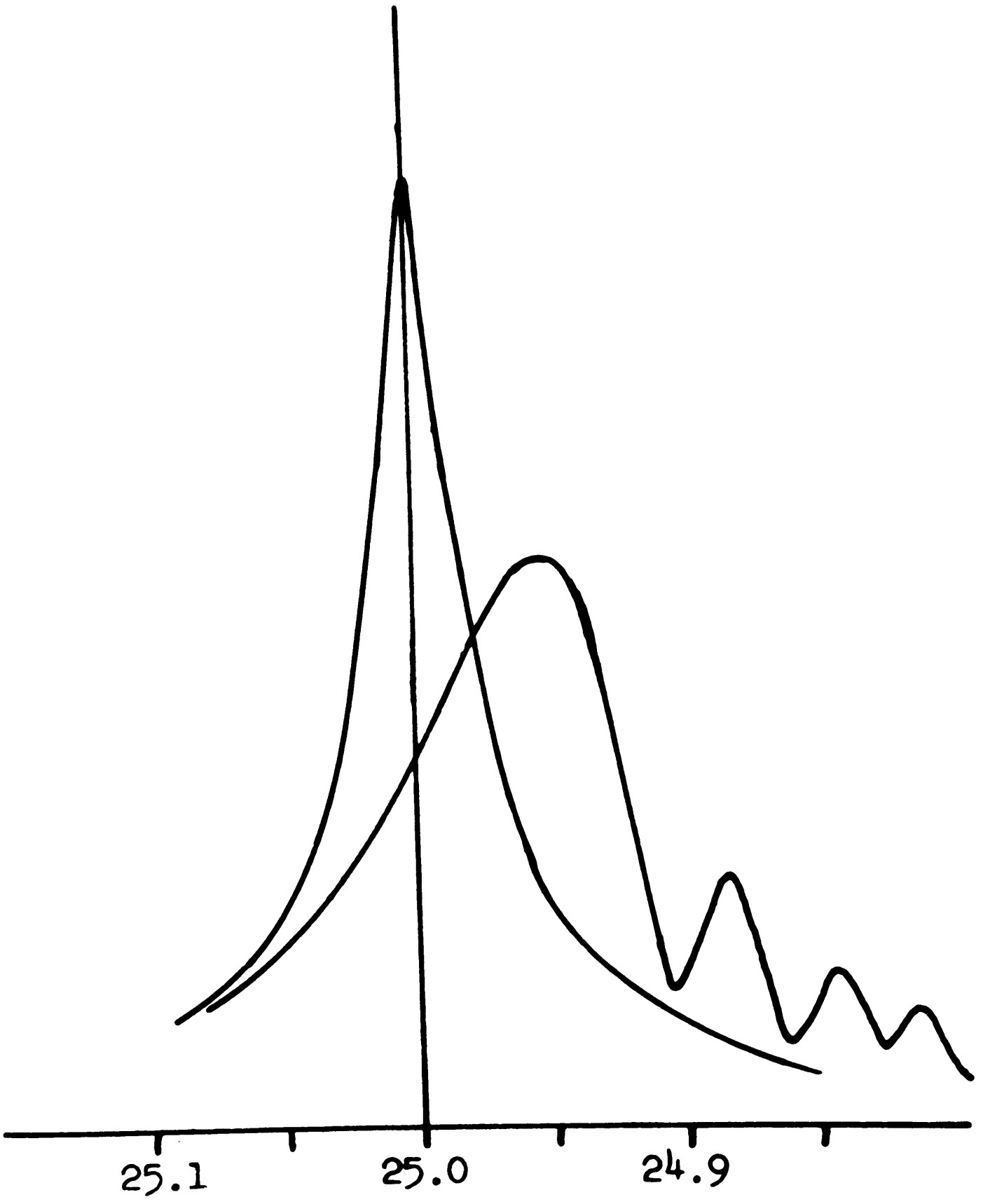

Fig. 14.
Response of a resonant circuit to the f-m cyclotron signal compared to the steady state response. $Q \approx 1200$

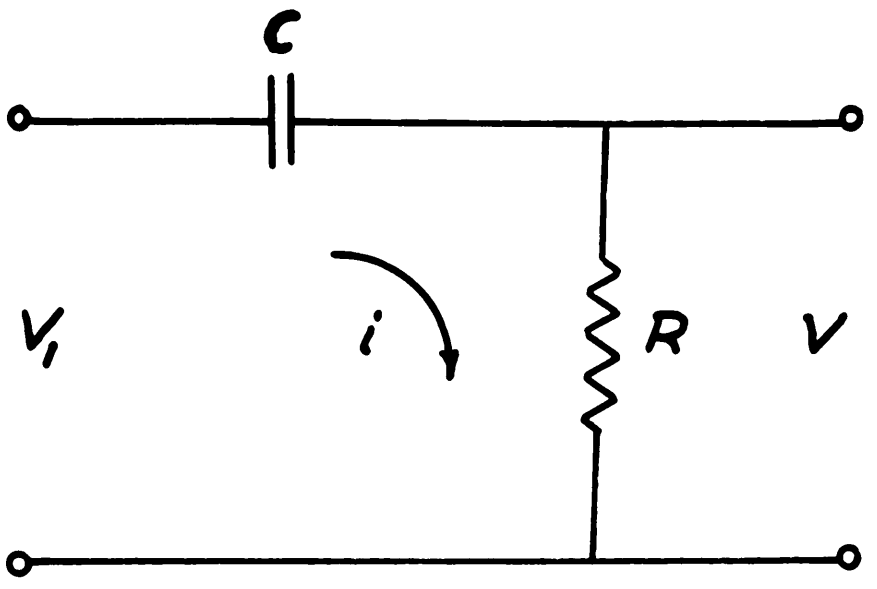

Fig.15(a)

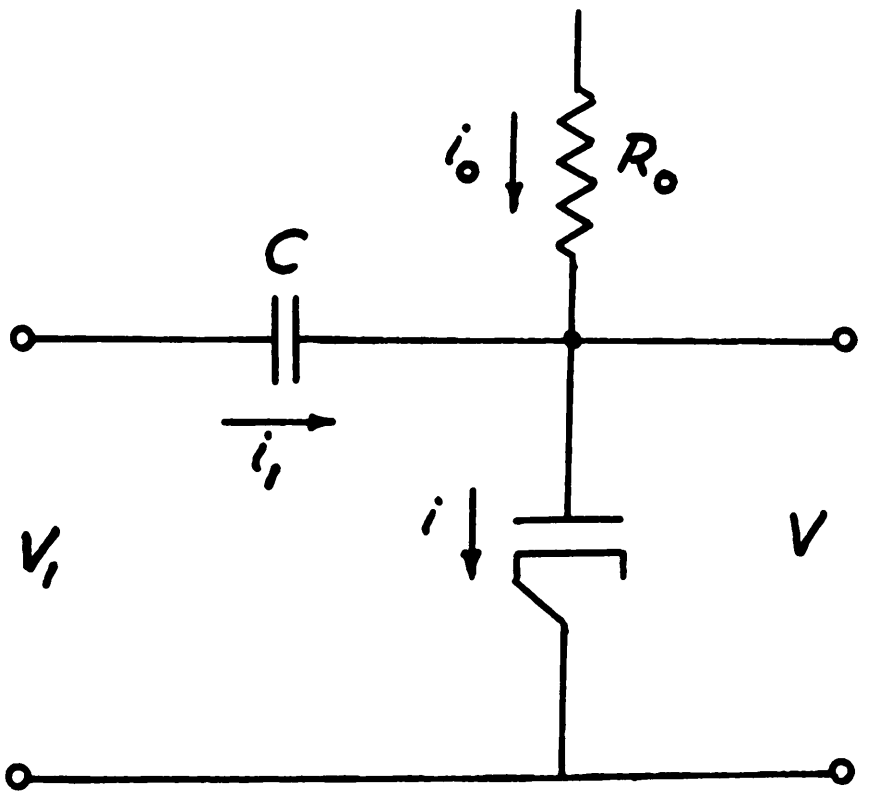

Fig.15(b).

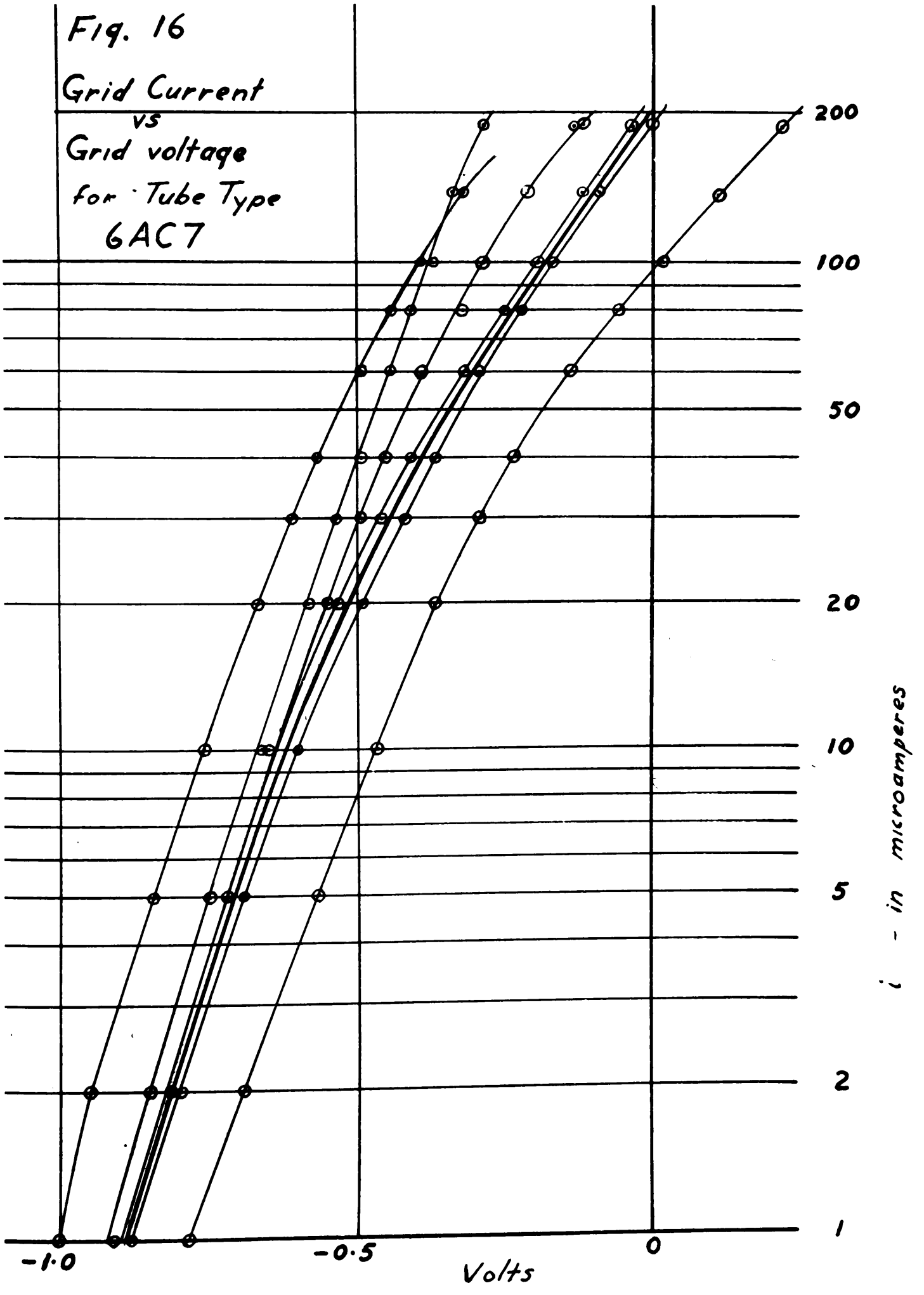
Fig. 16
Grid Current
vs
Grid voltage
for Tube Type
6AC7
200
100
50
20
10
5
2
1
i - in microamperes
-1.0
-0.5
0
Volts

McGILL UNIVERSITY LIBRARY
IXM IJ12.1950
★
UNACC.